Antigenic escape selects for the evolution of higher pathogen transmission and virulence

Akira Sasaki[1,2], Sébastien Lion[3] and Mike Boots[4,5*]

[1] Department of Evolutionary Studies of Biosystems, The Graduate University of Advanced Studies, SOKENDAI, Hayama, Kanagawa 2400139, Japan.

[2] Evolution and Ecology Program, International Institute for Applied Systems Analysis, Schlosplatz 1, A-2361, Laxenburg, Austria

[3] CEFE, CNRS, Univ Montpellier, EPHE, IRD, Montpellier, France.

[4] Integrative Biology, University of California, Berkeley, USA. CA 94720. Email: mboots@berkeley.edu

[5] Biosciences, University of Exeter, Penryn Campus, UK. TR10 9FE.

*corresponding author

Abstract

Despite the propensity for complex and non-equilibrium dynamics in nature, eco-evolutionary analytical theory typically assumes that populations are at equilibria. In particular pathogens often show antigenic escape from host immune defense, leading to repeated epidemics, fluctuating selection and diversification, but we do not understand how this impacts the evolution of virulence. We model the impact of antigenic drift and escape on the evolution of virulence in a generalized pathogen and apply a recently introduced oligomorphic methodology that captures the dynamics of the mean and variance of traits, to show analytically that these non-equilibrium dynamics select for the long-term persistence of more acute pathogens with higher virulence. Our analysis predicts both the timings and outcomes of antigenic shifts leading to repeated epidemics and predicts the increase in variation in both antigenicity and virulence before antigenic escape. There is considerable variation in the degree of antigenic escape that occurs across pathogens and our results may help to explain the difference in virulence between related pathogens including, potentially, human influenzas. Furthermore, it follows that these pathogens will have a lower R_0 with clear implications for epidemic, endemic behavior and control. More generally our results show the importance of examining the evolutionary consequences of non-equilibrium dynamics.

Key Words: Cross immunity, disease emergence, virulence, immunity, antigenic escape, transient evolution, adaptive dynamics, quantitative genetics, population genetics.

Introduction

Infectious disease remains a major problem for human health and agriculture [1–4] and are increasingly recognized as important in ecosystems and conservation [5,6]. This has led to the development of extensive theoretical literature on the epidemiology, ecology and evolution of host-pathogen interactions [7–10]. Understanding the drivers of the evolution of virulence, typically defined in the evolutionary literature as the increased death rate of individuals due to infection, is a key motivator of this theoretical work [8,10–14]. Generally, models assume that a higher transmission rate trade-offs against the intrinsic cost of reducing the infectious period due to higher death rates (virulence), and classically predict the evolution of a virulence that maximizes the parasite epidemiological R_0 [8,10–14]. In fact, this result only holds in models where ecological feedbacks take a constrained form, such that even relatively simple processes such as density-dependent mortality, multiple infections and spatial structure may lead to diversification or different optima [10,12,13,15]. Moreover, this classic evolutionary theory examines the long-term equilibrium evolutionary outcome in the context of stable endemic diseases, but in nature, infectious diseases often exhibit complex dynamics, with potentially important impacts on pathogen fitness [16–19].

Antibody-mediated immunity is a critical factor driving the dynamics of important infectious diseases such as seasonal influenza, leading to selection for novel variants that can escape immunity to the current predominant variant [20–22]. Such antigenic escape typically causes the optimal variant of the parasite to change through time as it moves through antigenic space. Moreover, partial cross-immunity between the different parasite variants may lead to recurrent epidemics, fluctuations in parasite variants and potentially

variant coexistence [23–26]. Previous theory has shown that the evolution of immune escape can lead to dramatic disease outbreaks [24–26], but the implications of these epidemiological dynamics for the evolution of disease virulence are unknown. This question is challenging in part because much of the theoretical framework used to study virulence evolution typically considers diseases that are at an endemic equilibrium [8,10–14]. As such we currently lack a broad theoretical understanding of the evolution of virulence in the presence of antigenic escape, despite its importance as an epidemic process and the likely implications of its inherently dynamical epidemic nature.

Here, we examine the impact of antigenic escape on the evolution of infectious disease in the context of the well-studied transmission/virulence trade-off [10,27]. We first examine analytically the case without cross-immunity and then apply a recently introduced 'oligomorphic' analysis that combines quantitative genetic and game theoretical approaches [28] to examine the impact of antigenic jumps and epidemic outbreaks due to cross immunity. Specifically, the oligomorphic analysis explicitly models not only changes in the mean trait but also changes in the variance of the trait. This variance is critical to the evolutionary outcome under non-equilibrium dynamics and the approach allows us to model the evolutionary dynamics of populations with multiple peaks in the character distribution. This analysis can be applied across a range of ecological and evolutionary time scales and allows us to examine evolutionary outcomes under non-equilibrium conditions. Our key result is that antigenic escape selects for higher transmission and virulence due to the repeated epidemics caused by immune escape, leading to the long-term persistence of acute pathogens. Indeed, antigenic escape has the potential to select for

infectious diseases with substantially higher virulence than that predicted by the maximization of R_0 in classic disease models.

Results

In order to tractably model antigenic escape with multiple variants and cross-immunity we follow the simplifying approaches of Gog and Grenfell [26]. Effectively the role of cross-immunity is to generate protection against becoming infectious with variants not yet encountered. In particular we assume that cross-immunity reduces the transmissibility of, rather than the susceptibility to, future variants. Furthermore, we assume that there is polarizing immunity, such that cross-immunity results in a proportion of individuals being completely immune. These assumptions allow tractability and have been shown not to impact the predictions of the model [26]. Specifically, we consider a population of pathogens structured by a one-dimensional antigenic trait x, so that $I(t,x)$ is the density of hosts infected with antigenicity variant x at time t. Following Gog and Grenfell [26], we assume that an individual is either perfectly susceptible or perfectly immune to a variant. A variant of pathogen can infect any host, but will be infectious only when the host is susceptible to that variant. When a variant y of pathogen infects a host that is susceptible to a variant x, the host may become (perfectly) immune to the variant x with probability $\sigma(x-y)$. This is the partial cross immunity function between variants x and y, that takes a value between 0 and 1 and is a decreasing function of antigenic distance $|x-y|$ between variants x and y. The density of hosts susceptible to antigenicity variant x at time t is noted $S(t,x)$.

Assuming that all pathogen variants have the same transmission rate β and virulence α, we can describe the dynamics with the following structured Susceptible-Infected-Recovered model:

$$\frac{\partial S(t,x)}{\partial t} = -\beta S(t,x) \int_{-\infty}^{\infty} \sigma(x-y) I(t,y)\, dy, \tag{1a}$$

$$\frac{\partial I(t,x)}{\partial t} = [\beta S(t,x) - (\gamma + \alpha)] I(t,x) + D \frac{\partial^2 I(t,x)}{\partial x^2}. \tag{1b}$$

where γ is the recovery rate, and $D = \mu\sigma_m^2/2$ is the diffusion constant due to random mutation in the continuous antigenic space, which is defined by one half of the mutation variance $\mu\sigma_m^2$, where μ is the mutation rate and σ_m^2 is the variance in the difference between parental and mutant traits [29,30]. The dynamics for the density of recovered hosts is omitted from (1) as it does not affect the dynamics (1) of the densities of susceptible and infected hosts.

Invasion of a single pathogen: in our first scenario, we start with a population where all hosts are susceptible to any variant ($\boldsymbol{S(0,x) = 1}$) and a small number of hosts infected by pathogen variant with antigenicity trait $\boldsymbol{x = 0}$ is initially introduced. The system then exhibits travelling wave dynamics in antigenicity space. At the front of the travelling wave, $\boldsymbol{I(t,x)}$ is sufficiently small and $\boldsymbol{S(t,x)}$ is sufficiently close to 1. Eq. (1a) can then be linearized as

$$\frac{\partial I(t,x)}{\partial t} = r I(t,x) + D \frac{\partial^2 I(t,x)}{\partial x^2} \tag{2}$$

where $r = \beta - (\gamma + \alpha)$ is the rate of increase of an antigenicity variant before it spreads in the population and causes the build-up of herd immunity. The system (1) asymptotically approaches travelling waves of both pathogen antigenicity distributions $I(t,x)$, which have

an isolated peak around the current antigenicity, and host susceptibility profile $S(t,x)$, that smoothly steps down towards a low level after the pathogen antigenicity distribution passes through, with a common constant wave speed [32] (Fig. 1a)

$$v = 2\sqrt{rD} = 2\sqrt{\big(\beta - (\gamma + \alpha)\big)D}. \quad (3)$$

As the width of the partial cross-immunity function $\sigma(x-y)$ increases, the travelling wave with static shapes described above is destabilized (Extended Data Fig. 1), and the system shows intermittent outbreaks that occur periodically both in time and in antigenicity space [26,32] (Fig. 1b). However, the wave speed is unchanged from (3), as the linearized system (2) towards the frontal end remains the same irrespective of the stability of wave profile that lags behind (Extended Data Fig. 1).

Evolution of antigenic escape with cross-immunity: To predict how cross-immunity affects the evolution of antigenic escape, we use an oligomorphic dynamics analysis [28]. In this analysis we consider a population composed of different antigenicity 'morphs' that can be seen as quasispecies. Specifically, we use the term 'morph' to describe the phenotypic trait mean and the continuous variance around this mean. The analysis in the methods allows us to track the dynamics of morph frequencies, p_i, and mean trait values, $\bar{x}_i$, as:

$$\frac{dp_i}{dt} = \beta(\bar{s}_i - \bar{s})p_i, \quad (4a)$$

$$\frac{d\bar{x}_i}{dt} = V_i \beta s'(\bar{x}_i). \quad (4b)$$

where $s(x)$ is the susceptibility profile of the population, which depends on the cross-immunity function σ, $\bar{s}_i$ is the mean susceptibility perceived by viral morph i, and $\bar{s}$ the

mean susceptibility averaged over the different viral morphs. Note that, in general, $s(x)$, $\bar{s}_i$ and $\bar{s}$ will be functions of time, as the susceptibility profile is molded by the epidemiological dynamics of $S(t,x)$ and $I(t,x)$.

Equation (4a) reveals that, as intuitively expected, morph i will increase in frequency if the susceptibility of the host population to this variant is higher on average. Equation (4b) shows that the increase in the mean antigenicity trait of morph i depends on (i) the variance of the morph distribution, V_i, (ii) the transmission rate, and (iii) the slope of the susceptibility profile close to the morph mean $\bar{x}_i$. Together with an equation for the dynamics of variance under mutation and selection (see Methods), equations (4a) and (4b) allow us to quantitatively predict the change in antigenicity after a primary outbreak, as shown in Fig. 2.

For instance, after a primary outbreak caused by a variant with antigenicity $\bar{x}_0 = 0$ at $t = 0$, the susceptibility profile is approximately constant and given by $s(x) = (1 - \psi_0)^{\sigma(x)}$, where ψ_0 is the final size of the epidemic of the primary outbreak at antigenicity $x = 0$ (see Methods). Thus, for a decreasing cross-immunity function, $\sigma(x)$, the slope of the susceptibility profile is positive, which selects for increased values of the mean antigenicity trait $\bar{x}_1$ of a second emerging morph (see Methods). As the process repeats itself, this leads to successive jumps in antigenic space. In addition, a more peaked cross-immunity function, σ, yields larger slopes to the susceptibility profile and thus selects for higher values of the antigenicity trait.

Long-term joint evolution of antigenicity, transmission and virulence: We now extend our analysis to account for mutations affecting pathogen life-history traits such as transmission and virulence. To simplify, we use the classical assumption of a transmission-virulence trade-off [8,10–14] and consider that a pathogen morph, $\boldsymbol{i}$, has frequency, $\boldsymbol{p_i}$, mean antigenicity trait, $\boldsymbol{\bar{x}_i}$, and mean virulence $\boldsymbol{\bar{\alpha}_i}$. In the methods, we show that the morph's mean traits change as

$$\frac{d}{dt}\begin{pmatrix}\bar{x}_i\\ \bar{\alpha}_i\end{pmatrix} = \mathbf{G}_i\begin{pmatrix}\beta(\bar{\alpha}_i)s'(\bar{x}_i)\\ \beta'(\bar{\alpha}_i)s(\bar{x}_i) - 1\end{pmatrix}$$

where $\mathbf{G_i}$ is the genetic (co)variance matrix, and the vector on the right-hand side is the selection gradient. Note that, while the selection gradient on antigenicity depends on the slope of the antigenicity profile at the morph mean, the selection gradient on virulence depends on the slope of the transmission-virulence trade-off at the morph mean, weighted by the susceptibility profile at the morph mean.

Assuming we can neglect the build-up of correlations between antigenicity and virulence due to mutation and selection, the genetic (co)variance matrix is diagonal with elements V_i^x and V_i^α. Then, as shown previously, antigenicity increases if the slope of the susceptibility profile is locally positive, while mean virulence increases as long as $\beta'(\bar{\alpha}_i) > 1/s(\bar{x}_i)$. For a fixed antigenicity trait, $x = x^*$, the susceptibility profile converges towards $s(x^*) = (\gamma + \alpha)/\beta$ and the evolutionary endpoint satisfies

$$\beta'(\alpha) = \frac{\beta(\alpha)}{\gamma + \alpha}$$

which corresponds to the classical result of R_0 maximisation for the unstructured SI model [15,27]. However, when antigenicity can evolve, selection will also lead to the build-up of a

184 positive covariance C between antigenicity and virulence, resulting in a synergistic effect
185 (Methods). As the antigenicity trait increases, the evolutionary trajectory of virulence
186 converges to the solution of

187 $$\beta'(\alpha) = 1$$

188 which corresponds to maximizing the rate of increase of pathogen $r(\alpha) = \beta(\alpha) - (\gamma + \alpha)$
189 in a fully susceptible population. This is equivalent to maximizing the wave speed $v(\alpha) =$
190 $2\sqrt{r(\alpha)D}$, as shown in the methods. Fig. 3a shows that, in the absence of cross-immunity,
191 the ES virulence is well predicted by r maximization. With cross-immunity (Fig. 3b),
192 virulence evolution is characterized by jumps that reflect the sudden shifts in antigenicity
193 due to cross-immunity.

194 As such antigenic escape selects for higher transmission and virulence and more acute
195 infectious diseases. This has parallels with the results that show that there is a transient
196 increase in virulence at the start of an epidemic with r rather than R_0 being maximized
197 [16,17,19,33], but here we predict the long-term persistence of highly transmissible and virulent
198 disease variants due to antigenic escape.

199 Although we have so far assumed a never-ending antigenic escape process, it is easy to
200 extend our analysis to consider that antigenic escape is constrained by pleiotropic effects.
201 Then, once the antigenicity trait has stabilized, the ES virulence would satisfy

202 $$\beta'(\alpha) = \frac{1 - \rho\, \beta(\alpha) s'(x)}{s(x)}$$

where $\rho = C/V_\alpha$ measures the correlation between antigenicity and virulence. Thus, the slope to the transmission-virulence trade-off at the ESS now takes an intermediate value between $\beta/(\gamma + \alpha)$ and 1, as shown in Fig. 4.

Short-term joint evolution of antigenicity and virulence: Although our analysis allows us to understand the long-term evolution of pathogen traits, it can also be used to accurately predict the short-term dynamics of antigenicity and virulence. We now consider that a primary outbreak has molded a susceptibility profile $s(x)$ that we assume constant. Although this assumption will cause deviations from the true susceptibility profile, it allows us to decouple our evolutionary oligomorphic dynamics from the epidemiological dynamics. Fig. 5 shows that the approximation accurately predicts the jump in antigenic space and joint increase in virulence during the secondary outbreak. The accuracy of the prediction depends on the time at which we seed the oligomorphic dynamical system, as detailed in the methods, but remains high for a broad range of values of this initial time. Hence, our analysis can be used to successfully predict the trait dynamics after the emergence of a new antigenic variant. Simulations show that this result is not dependent on the assumption of one dimensional antigenic space (Supplementary Information).

Discussion

We have shown how antigenic escape selects for more acute infectious diseases with higher transmission rates that cause increased mortality (virulence) in infected hosts. This result is important given the number of major infectious diseases such as seasonal influenza that have epidemiology driven by antigenic escape. Until recently the evolution of virulence literature has mostly focused on equilibrium solutions that in simple models lead to the classic idea that pathogens evolve to maximize their basic reproductive number R_0 [8,10–14]. Our results show that the process of antigenic escape leading to the continual replacement of variants [23–26], creates a dynamical invasion process that in and of itself selects for more acute, fast transmitting, highly virulent variants that do not maximize R_0. This has parallels with the finding that more acute variants are selected transiently at the start of epidemics [24-26], but critically, in our case the result is not a short-term transient outcome. Rather, the eco-evolutionary process leads to the long-term persistence of more acute variants. As such, antigenic escape may be an important driver of high virulence in infectious disease.

In the simpler case where there is no cross immunity, there is a travelling wave of new variants invading due to antigenic escape. In this case we can use established methods to gain analytical results that not only predict the speed of change of the variants, but also the evolutionarily stable virulence. With our model's assumptions, without antigenic escape we would get the classic result of the maximization of the reproductive number R_0 [8,10–14], but once there is antigenic escape we show analytically that the intrinsic growth rate of the infectious disease r is maximized. Maximizing the intrinsic growth rate leads to selection for higher transmission and in turn higher virulence. Effectively this is the equivalent of an infectious disease "live fast, die young" strategy. The outcome is due to the dynamical

replacement of variants, with new variants invading the population continually leading to a continual selection for the variants that invade better [24-26]. As such we predict that any degree of antigenic escape will in general select for more acute faster transmitting variants with higher virulence in the presence of a transmission-virulence trade-off. Although such a trade-off is a classical assumption in evolutionary epidemiology, it would be interesting to examine the impact of antigenic escape under different assumptions.

Partial cross-immunity leads to a series of jumps in antigenic space that are characteristic of the epidemiology of a number of diseases and in particular of the well-known dynamics of influenza A in humans [23–26]. Here a cloud of variants remains in antigenic space until there is a jump that, on average, overcomes the cross immunity and leads to the invasion of a new set of variants that are distant enough to escape the immunity of the resident variants [23–26]. In order to examine the evolutionary outcome in this scenario we applied a novel oligomorphic analysis [28] and again we find that antigenic escape selects for higher virulence toward the maximization of the intrinsic growth rate r. Both our analysis and simulations show that in the long term the virulence increases until it reaches a new optimum potentially of an order of magnitude higher than would be expected by the classic prediction of maximizing R_0. Therefore, antigenic escape whether it is through a continuous wave of antigenic drift or through large jumps, selects for higher virulence. We therefore expect this result to apply across the wide range of 'jumpiness' that we see across different viruses between these two extremes of continuous drift and punctuated jumps. We show that virulence increases after each antigenic jump, falling slightly at the next jump before increasing again until it reaches this new equilibrium. It is also important to note that the diversity within the morph increases in both antigenicity and virulence as we

move towards the next epidemic, reaching a maximum just at the point when the jump occurs. This increase in diversity could in principle be used as a predictor of the next jump in antigenic space.

Clearly the virulence of any particular infectious disease depends on multiple factors, including both host and parasite traits, and critically the relationship between transmission and virulence. This makes comparisons of the virulence across different infectious diseases problematic since the specific trade-off relationship between transmission and virulence is often unknown. However, our model shows that antigenic escape will, all things being equal, be a driver of higher virulence favoring more acute variants. It is also important to note that since antigenic escape is a very general mechanism that selects for higher virulence it follows that we may see high virulence in parasites even when the costs in terms of reduced infectious period are substantial. Amongst the influenzas, although there is a paucity of data, influenza C does not show obvious antigenic escape and is typically much less virulent than the other influenzas [34]. Furthermore, influenza A/H3 tends to show much more antigenic escape than influenza B and influenza A/H1 and again in line with our predictions typically influenza A/H3N2 is the more virulent [35,36]. It is important to note that these differences can be ascribed to multiple factors including circumvention of vaccination and that cross-immunity may itself directly impact disease severity. Furthermore the higher virulence of influenza A is often posited to be due to a more recent zoonotic emergence [37]. Moreover, direct comparisons between the rates of antigenic escape between influenza A/H1 and influenza B are difficult and clearly there are also highly virulent pathogens that do not show antigenic escape such as measles. Therefore, a formal comparative analysis is confounded by multiple factors. Nevertheless, our model suggests

288 that differences in the rates of antigenic escape of the different influenzas may impact their
289 virulence and the evidence from influenza is at least consistent with the predictions of the
290 model.

291 An important implication of our work is that antigenic escape selects for variants with a
292 higher virulence than the value that maximizes R_0 and therefore leads to the evolution of
293 infectious diseases with lower R_0. From this point of view, it may be naively concluded
294 that diseases with antigenic escape may be easier to eliminate and control with vaccination.
295 Of course, in practice the opposite is often true since producing an effective vaccine is
296 much more problematic when there is antigenic escape [38,39]. On the other hand with lower
297 R_0 epidemics will tend to be less explosive than they otherwise would have been, having a
298 lower peak but lasting longer, with evolution here effectively 'flattening the curve'.
299 Infectious diseases that show punctuated antigenic escape are characterized by repeated
300 epidemics, but our work suggests that due to the selection for a lower R_0 the eco-
301 evolutionary feedback will have significantly impacted the pattern of these epidemics.
302 More generally our results highlight how ecological/epidemiological dynamics can impact
303 evolutionary outcomes that in turn feedback into the epidemiology characteristics of the
304 disease.

305 We have used oligomorphic dynamics [28] to make predictions on the waiting times and
306 outcomes of the antigenic jumps in our model with cross immunity. This approach tracks
307 changes in both mean trait values and trait variances in models with explicit ecological
308 dynamics. As such it combines aspects of eco-evolutionary theory [40,41] and quantitative
309 genetics approaches [42,43] to provide a more complete understanding of the evolution of
310 quantitative traits. Our approach can take into account a wide range of different ecological

311 and evolutionary time scales and therefore allows us to address fundamental questions on
312 eco-evolutionary feedbacks and on the separation between ecological and evolutionary
313 time scales. This is important since it allows us to test the implications of the different
314 assumptions of classical evolutionary theory and to better understand the role of eco-
315 evolutionary feedbacks on evolutionary outcomes. Furthermore, the approach can be
316 applied widely to model transient dynamics, and to predict the waiting times and extent of
317 diversification that occurs in a range of contexts [28,44]. Moreover, antigenic evolution is
318 known to also lead to diversification and variant coexistence [45–48], and it would be
319 interesting to extend our analysis to these other evolutionary outcomes.

320 Our results emphasize that epidemiological dynamics may have important implications for
321 the evolution of infectious disease. To facilitate its broader application, the oligomorphic
322 methodology should be extended to structured populations and combined with stochastic
323 evolutionary theory in order to fully address the evolutionary dynamics of emerging
324 disease. Human coronaviruses can evolve antigenically to escape antibody immunity [49]
325 and it would be useful to apply our approaches to a more specific model of the SARS-Cov-
326 2 epidemic. In particular, our ability to predict the waiting time until the emergence of the
327 next antigenic cluster has the potential to be important in such applied contexts.

328 In principle epidemics of new variants that adapts to a novel host would display equivalent
329 dynamics to those described here for antigenic escape. It also follows that interventions
330 that impact epidemiological dynamics may also have impacts on the evolution of pathogen
331 traits such as virulence or transmission. Our results suggest that immune escape driven by
332 transmission blocking imperfect vaccination might also select for higher virulence in the
333 longer term [50,51], although these effects are likely overwhelmed by selection on transmission

in an emerging pandemic such as SARS-Cov-2 [52,53]. Furthermore, dynamical feedbacks are important in a range of contexts beyond infectious disease and our approach may help us examine the importance of interactions between frequency dependent 'stabilizing' and equalizing evolutionary drivers [54]. The oligomorphic analytical approaches we use here are therefore likely to be useful in understanding a wide range of dynamical evolutionary outcomes.

Methods

Oligomorphic dynamics of antigenic escape

We consider a model of the antigenic escape of a pathogen from host herd immunity on a one-dimensional antigenicity space (x). We track the changes in the density $S(t,x)$ of hosts that are susceptible to antigenicity variant x of pathogen at time t, and the density $I(t,x)$ of hosts that are currently infected and infectious with antigenicity variant x of pathogen at time t:

$$\frac{\partial S(t,x)}{\partial t} = -S(t,x)\int_{-\infty}^{\infty}\beta\sigma(x-y)I(t,y)\,dy, \tag{5}$$

$$\frac{\partial I(t,x)}{\partial t} = \beta S(t,x)I(t,x) - (\gamma+\alpha)I(t,x) + D\frac{\partial^2 I(t,x)}{\partial x^2}. \tag{6}$$

where β, α, and γ are the transmission rate, virulence (additional mortality due to infection), and recovery rate of pathogens which are independent of antigenicity. The function $\sigma(x-y)$ denotes the degree of cross immunity: a host infected by pathogen variant y acquires perfect cross immunity with probability $\sigma(x-y)$ but fails to acquire any cross immunity with probability $1-\sigma(x-y)$ (this is called polarized cross immunity by Gog and Grenfell [26]). The degree $\sigma(x-y)$ of cross-immunity is assumed to be a

decreasing function of the distance $|x-y|$ between variants x and y. When a new variant with antigenicity $x=0$ is introduced at time $t=0$, the initial host population is assumed to be susceptible to any antigenicity variant of pathogen: $S(0,x)=1$. In (6), $D=\mu\sigma_m^2/2$ is one half of the mutation variance for the change in antigenicity, representing random mutation in the continuous antigenic space.

Susceptibility profile molded by the primary outbreak. We first analyze the dynamics of the primary outbreak of a pathogen and derive the resulting susceptibility profile, which can be viewed as the fitness landscape subsequently experienced by the pathogen. For simplicity we assume that mutation can be ignored during the first epidemic initiated with antigenicity stain $\boldsymbol{x=0}$. The density $\boldsymbol{S_0(t)=S(t,0)}$ of hosts that are susceptible to the currently prevailing antigenicity variant $\boldsymbol{x=0}$, as well as the density $\boldsymbol{I_0(t)=I(t,0)}$ of hosts that are currently infected by the focal variant change with time as

$$\frac{dS_0}{dt}=-S_0\beta I_0, \tag{7}$$

$$\frac{dI_0}{dt}=S_0\beta I_0-(\gamma+\alpha)I_0, \tag{8}$$

$$\frac{dR_0}{dt}=\gamma I_0. \tag{9}$$

with $S_0(0)=1$, $I_0(0)\approx 0$, and $R_0(0)=0$. The final size of the primary outbreak,

$$\psi_0=R_0(\infty)=1-S_0(\infty)=\exp\left[-\beta\int_0^\infty I_0(t)\,dt\right],$$

is determined as the unique positive root of

$$\psi_0=1-e^{-\rho_0\psi_0}, \tag{10}$$

where $\rho_0 = \beta/(\gamma + \alpha) > 1$ is the basic reproductive number [7]. Associated with this epidemiological change, the susceptibility profile $S_x(t) = S(t, x)$ against antigenicity x ($x \neq 0$) other than the currently circulating variant ($x = 0$) changes by cross immunity as

$$\frac{dS_x}{dt} = -S_x \beta \sigma(x) I_0, \qquad (x \neq 0). \tag{11}$$

Integrating both sides of (11) from $t = 0$ to $t = \infty$, we see that the susceptibility profile $s(x) = S_x(\infty)$ after the primary outbreak at $x = 0$ is

$$s(x) = \exp\left[-\beta\sigma(x)\int_0^\infty I_0(t)\,dt\right] = (1 - \psi_0)^{\sigma(x)} = e^{-\rho_0 \sigma(x)\psi_0}, \tag{12}$$

where the last equality follows from (10). The susceptibility can be effectively reduced by cross-immunity when the primary variant has a large impact (i.e. when the fraction of hosts remaining uninfected, $1 - \psi_0$, is small) and when the degree of cross immunity is strong (i.e. when $\sigma(x)$ is close to 1). With a variant antigenically very close to the primary variant ($x \approx 0$), the cross immunity is very strong ($\sigma(x) \approx 1$) so that the susceptibility against variant x is nearly maximally reduced: $s(x) \approx 1 - \psi_0$. With a variant antigenically distant from the primary variant, $\sigma(x)$ becomes substantially smaller than 1, making the host more susceptible to the variant. For example, if the cross immunity is halved ($\sigma(x) = 0.5$) from its maximum value 1, then the susceptibility to that variant is as large as $(1 - \psi_0)^{0.5}$. If a variant is antigenically very distant from the primary variant, then $\sigma(x) \approx 0$, and the host is nearly fully susceptibility to the variant ($s(x) \approx 1$).

Threshold antigenic distance for escaping immunity raised by primary outbreak. Of particular interest is the threshold antigenicity distance $\boldsymbol{x_c}$ that allows for antigenic escape, i.e. any antigenicity variant more distant than this threshold from the primary variant ($\boldsymbol{x > x_c}$) can increase when introduced after the primary outbreak. Such a threshold is determined from

$$\frac{\beta s(x_c)}{\gamma + \alpha} = \rho_0 s(x_c) = 1$$

or

$$s(x_c) = (1 - \psi_0)^{\sigma(x_c)} = e^{-\rho_0 \sigma(x_c)\psi_0} = \frac{1}{\rho_0}, \tag{13}$$

where we used (12). With a specific choice of cross-immunity profile,

$$\sigma(x) = \exp\left[-\frac{x^2}{2\omega^2}\right], \tag{14}$$

the threshold antigenicity beyond which the virus can increase in the susceptibility profile $s(x)$ after the primary outbreak is obtained, by substituting (14) into (13)

$$\exp\left[-\rho_0 \psi_0 \exp\left[-\frac{x_c^2}{2\omega^2}\right]\right] = \frac{1}{\rho_0},$$

and taking logarithm of both sides twice:

$$x_c = \omega \sqrt{2 \log \frac{\rho_0 \psi_0}{\log \rho_0}}. \tag{15}$$

Oligomorphic dynamics. Integrating both sides of (6) over the whole space, we obtain the dynamics for the total density of infected hosts, $\bar{\boldsymbol{I}}(\boldsymbol{t}) = \int_{-\infty}^{\infty} \boldsymbol{I}(\boldsymbol{t},\boldsymbol{x})\boldsymbol{dx}$:

$$\frac{d\bar{I}}{dt} = \left[\beta \int_{-\infty}^{\infty} S(t,x)\phi(t,x)\,dx - (\gamma+\alpha)\right]\bar{I}(t) = [\beta\bar{S}(t) - (\gamma+\alpha)]\bar{I}(t). \qquad (16)$$

where

$$\phi(t,x) = I(t,x)/\bar{I}(t),$$

is the relative frequency of antigenicity variant x in the pathogen population circulating at time t, and

$$\bar{S}(t) = \int_{-\infty}^{\infty} S(t,x)\phi(t,x)\,dx \qquad (17)$$

is the mean susceptibility experienced by currently circulating pathogens. The dynamics for the relative frequency $\phi(t,x)$ of pathogen antigenicity is

$$\frac{\partial\phi}{\partial t} = \beta\{S(t,x) - \bar{S}(t)\}\phi(t,x) + D\frac{\partial^2\phi}{\partial x^2}. \qquad (18)$$

As in Sasaki and Dieckmann [28], we decompose the frequency distribution to the sum of several morph distributions (oligomorphic decomposition) as

$$\phi(t,x) = \sum_i p_i\phi_i(t,x) \qquad (19)$$

where $p_i(t)$ is the frequency of morph i and $\phi_i(t,x)$ is within-morph distribution of antigenicity. By definition, $\sum_i p_i = 1$ and $\int_{-\infty}^{\infty}\phi_i(t,x)\,dx = 1$. Let

$$\bar{x}_i = \int_{-\infty}^{\infty} x\phi_i(t,x)\,dx \qquad (20)$$

be the mean antigenicity of a morph and

$$V_i = \int_{-\infty}^{\infty} (x - \bar{x}_i)^2 \phi_i(t,x)\, dx = O(\epsilon^2). \quad (21)$$

be the within-morph variance of each morph, which is assumed to be small, of the order of ϵ^2. Let us denote the mean susceptibility of host population for viral morph i by $\bar{S}_i = \int_{-\infty}^{\infty} S(t,x)\phi_i(t,x)\, dx$. As shown in Sasaki and Dieckmann [28], the dynamics for viral morph frequency is expressed as

$$\frac{dp_i}{dt} = \beta(\bar{S}_i - \bar{S})p_i + O(\epsilon), \quad (22)$$

while the dynamics for the within-morph distribution of antigenicity is

$$\frac{\partial \phi_i}{\partial t} = \beta\{S(t,x) - \bar{S}_i\}\phi_i(t,x) + D\frac{\partial^2 \phi_i}{\partial x^2}. \quad (23)$$

From this, the dynamics for the mean antigenicity of a morph,

$$\frac{d\bar{x}_i}{dt} = V_i \beta \left.\frac{\partial S}{\partial x}\right|_{x=\bar{x}_i} + O(\epsilon^3). \quad (24)$$

and the dynamics for the within-morph variance of a morph

$$\frac{dV_i}{dt} = \frac{1}{2}\beta \left.\frac{\partial^2 S}{\partial x^2}\right|_{x=\bar{x}_i} \{E[\xi_i^4] - V_i^2\} + 2D + O(\epsilon^5). \quad (25)$$

are derived, where $\xi_i = x - \bar{x}_i$ and $E[\xi_i^4] = \int_{-\infty}^{\infty}(x - \bar{x}_i)^4 \phi_i(t,x)dx$ is the fourth central moment of antigenicity around the morph mean. Assuming that the within-morph distribution is normal (Gaussian closure), $E[\xi_i^4] = 3V_i^2$ and hence Eq. (25) becomes

$$\frac{dV_i}{dt} = \beta \left.\frac{\partial^2 S}{\partial x^2}\right|_{x=\bar{x}_i} V_i^2 + 2D + O(\epsilon^5). \quad (26)$$

Second outbreak predicted by OMD. Equations (22), (24) and (26) are general, but they rely on a full knowledge of the dynamics of the susceptibility profile $\mathbf{S}(\mathbf{t},\mathbf{x})$. In order to make further progress, we use an additional approximation by substituting Eq. (13), the susceptibility profile over viral antigenicity space after the primary outbreak at $\mathbf{x}=\mathbf{0}$ and before the onset of the second outbreak at a distant position. We keep track of two morphs at positions $\mathbf{x_0}(\mathbf{t})$ and $\mathbf{x_1}(\mathbf{t})$, where the first morph is that caused the primary outbreak at $\mathbf{x}=\mathbf{0}$, and the second morph is that emerged in the range $\mathbf{x}>\mathbf{x_c}$ beyond the threshold antigenicity $\mathbf{x_c}$ defined in Eq. (13) (and (15) for a specific form of $\boldsymbol{\sigma}(\mathbf{x})$) as the source of the next outbreak.

As $s(x)=(1-\psi_0)^{\sigma(x)}=\exp[\sigma(x)\log(1-\psi_0)]$, we have

$$\frac{\mathrm{d}s}{\mathrm{d}x}(\bar{x}_i)=\left[\frac{\mathrm{d}\sigma}{\mathrm{d}x}(\bar{x}_i)\log(1-\psi_0)\right]s(\bar{x}_i),$$

and

$$\frac{\mathrm{d}^2s}{\mathrm{d}x^2}(\bar{x}_i)=\left[\frac{\mathrm{d}^2\sigma}{\mathrm{d}x^2}(\bar{x}_i)\log(1-\psi_0)+\left\{\frac{\mathrm{d}\sigma}{\mathrm{d}x}(\bar{x}_i)\log(1-\psi_0)\right\}^2\right]s(\bar{x}_i).$$

Therefore, the frequency, mean antigenicity, and variance of antigenicity of an emerging morph ($i=1$) change respectively as

$$\begin{aligned}\frac{dp_1}{dt}&=\beta[s(\bar{x}_1)-s(\bar{x}_0)]p_1(1-p_1),\\ \frac{d\bar{x}_1}{dt}&=V_1\beta\frac{\mathrm{d}s}{\mathrm{d}x}(\bar{x}_1),\\ \frac{dV_1}{dt}&=\beta\frac{\mathrm{d}^2s}{\mathrm{d}x^2}(\bar{x}_1)V_1^2+2D,\end{aligned}\qquad(27)$$

The predicted change in the mean antigenicity is plotted by integrating Eq. (27). As initial condition, we choose the time when a seed of second peak in the range $x > x_c$ first appears, and then compute the mean trait as

$$\bar{x}(t) = x_0\big(1 - p_1(t)\big) + \bar{x}_1 p_1(t). \tag{28}$$

In the case of Fig. 2, where $\beta = 2, \gamma + \alpha = 0.6, D = 0.001$, and $\omega = 2$, the final size of epidemic for the primary outbreak, defined as (7) was $\psi = 0.959$, and the critical antigenic distance for the increase of pathogen variant obtained from (26) was $x_c = 2.795$. The initial condition for the oligomorphic dynamics (27) for the second morph was then $p_1(t_0) = 1.6 \times 10^{-8}$, $\bar{x}_1(t_0) = 3.239$, $V_1(t_0) = 0.2675$ at $t_0 = 41$. In Fig. 2, the predicted trajectory for the mean antigenicity (28) is plotted as a red curve, together with the mean antigenicity change observed in simulation (blue curve).

The accuracy of predicting with OMD the antigenicity and the timing of the second outbreak. Here we describe how we define the initial conditions for oligomorphic dynamics, i.e., the frequency, the mean antigenicity and the variance in antigenicity of the morph that caused the primary outbreak and the morph which may cause the second outbreak. We then show how the accuracy in prediction of the second outbreak depends on the timing of the prediction.

We divide the antigenicity space into two at $x = x_c$ above which the pathogen can increase under the given susceptibility profile after the primary outbreak, but below which the pathogen cannot increase. We then take relative frequencies of pathogens above x_c and below x_c, and the conditional mean and variance in these separated regions to set the initial

frequencies, means, and variances of the morphs at the time t_0 when we start integrating the oligomorphic dynamics to predict the second outbreak:

$$
\begin{aligned}
p_0(t_0) &= \frac{\int_0^{x_c} I(t_0,x)\,dx}{\int_0^{\infty} I(t_0,x)\,dx}, & p_1(t_0) &= \frac{\int_{x_c}^{\infty} I(t_0,x)\,dx}{\int_0^{\infty} I(t_0,x)\,dx},\\
\bar{x}_0(t_0) &= \frac{\int_0^{x_c} xI(t_0,x)\,dx}{\int_0^{x_c} I(t_0,x)\,dx}, & \bar{x}_1(t_0) &= \frac{\int_{x_c}^{\infty} xI(t_0,x)\,dx}{\int_{x_c}^{\infty} I(t_0,x)\,dx},\\
V_0(t_0) &= \frac{\int_0^{x_c}\left(x-\bar{x}_0(t_0)\right)^2 I(t_0,x)\,dx}{\int_0^{x_c} I(t_0,x)\,dx}, & V_1(t_0) &= \frac{\int_{x_c}^{\infty}\left(x-\bar{x}_1(t_0)\right)^2 I(t_0,x)\,dx}{\int_{x_c}^{\infty} I(t_0,x)\,dx}.
\end{aligned}
\tag{29}
$$

We then compare the trajectory for mean antigenicity change observed in simulation (blue curve in Fig. 2) and the predicted trajectory (red curve in Fig. 2) for mean antigenicity (28) by integrating oligomorphic dynamics (27) with initial condition (29) at time $t = t_0$. Extended Fig. 2 shows how the accuracy of prediction, measured by the Kullback-Leibler divergence between these two trajectories depends on the timing $t_0$chosen for the prediction. The second outbreak occurs around t = 54.6 where mean antigenicity jumps from around 0 to around 5. The prediction with OMD is accurate if it is made for $t_0 > 40$. Fig. 2 is drawn for $t_0 = 41$ where the second peak is about to emerge (see Extended Data Fig. 2). Even for the latest prediction for $t_0 = 51$ in Extended Fig. 2, the morph frequency of the emerging second morph was only 0.3% off, so the prediction is still worthwhile to make.

Extended Data Fig. 2 shows that the prediction power is roughly constant (albeit with a wiggle) for $5 < t_0 < 30$ (the predicted timings are 10-15% longer than actual timing for $5 < t_0 < 30$), and steadily improved for $t_0 > 30$. When the prediction is made very early ($t_0 < 5$) the deviations are larger.

Oligomorphic dynamics for the joint evolution of antigenicity and virulence

Let $s(x)$ be the susceptibility of the host population against antigenicity x. A specific susceptibility profile is given by (12) with cross-immunity function $\sigma(x)$ and the final size ψ_0 of epidemic of the primary outbreak. Note that, as above, the susceptibility profile is in general a function of time. The density $I(x,\alpha)$ of hosts infected by a pathogen of antigenicity x and virulence α changes with time, when rare, as

$$\frac{\partial I(x,\alpha)}{\partial t} = \beta s(x) I(x,\alpha) - (\gamma + \alpha) I(x,\alpha) + D_x \frac{\partial^2 I}{\partial x^2} + D_\alpha \frac{\partial^2 I}{\partial \alpha^2}. \quad (30)$$

The change in the frequency $\phi(x,\alpha) = I(x,\alpha)/\int\int I(x,\alpha)dxd\alpha$ of a pathogen with antigenicity x and virulence α follows

$$\frac{\partial \phi}{\partial t} = \{w(x,\alpha) - \overline{w}\}\phi + D_x \frac{\partial^2 \phi}{\partial x^2} + D_\alpha \frac{\partial^2 \phi}{\partial \alpha^2}, \quad (31)$$

where

$$w(x,\alpha) = \beta(\alpha) s(x) - \alpha, \quad (32)$$

is the fitness of a pathogen with antigenicity x and virulence α and $\overline{w} = \int\int w(x,\alpha)dxd\alpha$ is the mean fitness.

Let us decompose the joint frequency distribution $\phi(x,\alpha)$ of the viral quasispecies as (oligomorphic decomposition):

$$\phi(x,\alpha) = \sum_i \phi_i(x,\alpha) p_i, \quad (33)$$

where $\phi_i(x,\alpha)$ is the joint frequency distribution of antigenicity x and virulence α in morph i ($\int\int \phi_i dx d\alpha = 1$) and p_i is the relative frequency of morph i ($\sum_i p_i = 1$). The frequency of morph i then changes as

$$\begin{aligned} \frac{dp_i}{dt} &= \left(\bar{w}_i - \sum_j \bar{w}_j p_j\right) p_i, \\ \frac{\partial \phi_i}{\partial t} &= (w(x,\alpha) - \bar{w}_i)\phi_i(x,\alpha) + D_x \frac{\partial^2 \phi_i}{\partial x^2} + D_\alpha \frac{\partial^2 \phi_i}{\partial \alpha^2}, \end{aligned} \tag{34}$$

where $\bar{w}_i = \int\int w(x,\alpha)\phi_i(x,\alpha)\, dx d\alpha$ is the mean fitness of morph i.

Assuming that the traits are distributed narrowly around the morph means $\bar{x}_i = \int\int x\phi_i(x,\alpha) dx d\alpha$ and $\bar{\alpha}_i = \int\int \alpha\phi_i(x,\alpha)\, dx d\alpha$, so that $\xi_i = x - \bar{x}_i = O(\epsilon)$ and $\zeta_i = \alpha - \bar{\alpha}_i = O(\epsilon)$ where ϵ is a small constant, we expand the fitness $w(x,\alpha)$ around the means $\bar{x}_i$ and $\bar{\alpha}_i$ of morph i,

$$\begin{aligned} w(x,\alpha) = w(\bar{x}_i, \bar{\alpha}_i) &+ \left(\frac{\partial w}{\partial x}\right)_i \xi_i + \left(\frac{\partial w}{\partial \alpha}\right)_i \zeta_i \\ &+ \frac{1}{2}\left(\frac{\partial^2 w}{\partial x^2}\right)_i \xi_i^2 + \left(\frac{\partial^2 w}{\partial x \partial \alpha}\right)_i \xi_i \zeta_i + \frac{1}{2}\left(\frac{\partial^2 w}{\partial \alpha^2}\right)_i \zeta_i^2 + O(\epsilon^3). \end{aligned}$$

Substituting this and

$$\bar{w}_i = w(\bar{x}_i, \bar{\alpha}_i) + \frac{1}{2}\left(\frac{\partial^2 w}{\partial x^2}\right)_i V_i^{xx} + \left(\frac{\partial^2 w}{\partial x \partial \alpha}\right)_i V_i^{x\alpha} + \frac{1}{2}\left(\frac{\partial^2 w}{\partial \alpha^2}\right)_i V_i^{\alpha\alpha} + O(\epsilon^3)$$

into (34), we have

$$\frac{dp_i}{dt} = \left[w_i - \sum_j w_j p_j \right] p_i + O(\epsilon), \tag{35}$$

$$\frac{\partial \phi_i}{\partial t} = \left[\left(\frac{\partial w}{\partial x}\right)_i \xi_i + \left(\frac{\partial w}{\partial \alpha}\right)_i \zeta_i + \frac{1}{2}\left(\frac{\partial^2 w}{\partial x^2}\right)_i (\xi_i^2 - V_i^x) + \left(\frac{\partial^2 w}{\partial x \partial \alpha}\right)_i (\xi_i \zeta_i - C_i) + \frac{1}{2}\left(\frac{\partial^2 w}{\partial \alpha^2}\right)_i (\zeta_i^2 - V_i^\alpha) \right] \phi_i + D_x \frac{\partial^2 \phi_i}{\partial x^2} + D_\alpha \frac{\partial^2 \phi_i}{\partial \alpha^2} + O(\epsilon^3). \tag{36}$$

where $w_i = w(\bar{x}_i, \bar{\alpha}_i)$, $\left(\frac{\partial w}{\partial x}\right)_i = \frac{\partial w}{\partial x}(\bar{x}_i, \bar{\alpha}_i)$, $\left(\frac{\partial w}{\partial \alpha}\right)_i = \frac{\partial w}{\partial \alpha}(\bar{x}_i, \bar{\alpha}_i)$, $\left(\frac{\partial^2 w}{\partial x^2}\right)_i = \frac{\partial^2 w}{\partial x^2}(\bar{x}_i, \bar{\alpha}_i)$, $\left(\frac{\partial^2 w}{\partial x \partial \alpha}\right)_i = \frac{\partial^2 w}{\partial x \partial \alpha}(\bar{x}_i, \bar{\alpha}_i)$, and $\left(\frac{\partial^2 w}{\partial \alpha^2}\right)_i = \frac{\partial^2 w}{\partial \alpha^2}(\bar{x}_i, \bar{\alpha}_i)$ are fitness and its first and second derivatives evaluated at the mean traits of morph i, and

$$\begin{aligned} V_i^x &= E_i[(x - \bar{x}_i)^2], \\ C_i &= E_i[(x - \bar{x}_i)(\alpha - \bar{\alpha}_i)], \\ V_i^\alpha &= E_i[(\alpha - \bar{\alpha}_i)^2], \end{aligned} \tag{37}$$

are within-morph variances and covariance of the traits of morph i. Here, $E_i[f(x,\alpha)] = \int\int f(x,\alpha)\phi_i(x,\alpha)\, dx\, d\alpha$ denotes taking expectation of a function f with respect to the joint trait distribution $\phi_i(x,\alpha)$ of morph i.

Substituting (36) into the change in the mean antigenicity of morph i

$$\frac{d\bar{x}_i}{dt} = \frac{d}{dt}\int\int x\phi_i(x,\alpha)\, dx\, d\alpha = \int\int x \frac{\partial \phi_i}{\partial t} dx\, d\alpha = \int\int (\bar{x}_i + \xi_i) \frac{\partial \phi_i}{\partial t} d\xi_i\, d\zeta_i,$$

we have

$$\frac{d\bar{x}_i}{dt} = \left(\frac{\partial w}{\partial x}\right)_i V_i^x + \left(\frac{\partial w}{\partial \alpha}\right)_i C_i + O(\epsilon^3). \tag{38}$$

Similarly, the change in the mean virulence of morph i is expressed as

$$\frac{d\bar{\alpha}_i}{dt} = \left(\frac{\partial w}{\partial x}\right)_i C_i + \left(\frac{\partial w}{\partial \alpha}\right)_i V_i^\alpha + O(\epsilon^3). \tag{39}$$

Equations (38)-(39) from the mean trait change is summarized in a matrix form as

$$\frac{d}{dt}\begin{pmatrix}\bar{x}_i\\ \bar{\alpha}_i\end{pmatrix} = \boldsymbol{G_i}\begin{pmatrix}\left(\frac{\partial w}{\partial x}\right)_i\\ \left(\frac{\partial w}{\partial \alpha}\right)_i\end{pmatrix} + O(\epsilon^3), \tag{40}$$

where

$$\boldsymbol{G_i} = \begin{pmatrix}V_i^x & C_i\\ C_i & V_i^\alpha\end{pmatrix} \tag{41}$$

is the variance-covariance matrix of the morph i.

Substituting (36) into the right-hand side of the change in variance of antigenicity of morph i,

$$\frac{dV_i^x}{dt} = \frac{d}{dt}\int\int \xi_i^2\,\phi_i\,d\xi_i d\zeta_i = \int\int \xi_i^2\frac{\partial \phi_i}{\partial t}d\xi_i d\zeta_i$$

and those in the change in the other variance and covariance, we have

$$\begin{aligned}
\frac{dV_i^x}{dt} &= \frac{1}{2}\left(\frac{\partial^2 w}{\partial x^2}\right)_i [E_i(\xi_i^4) - (V_i^x)^2] + \left(\frac{\partial^2 w}{\partial x \partial \alpha}\right)_i [E_i(\xi_i^3\zeta_i) - V_i^x C_i]\\
&\quad + \frac{1}{2}\left(\frac{\partial^2 w}{\partial \alpha^2}\right)_i [E_i(\xi_i^2\zeta_i^2) - V_i^x V_i^\alpha] + 2D_x + O(\epsilon^5),\\
\frac{dC_i}{dt} &= \frac{1}{2}\left(\frac{\partial^2 w}{\partial x^2}\right)_i [E_i(\xi_i^3\zeta_i) - V_i^x C_i] + \left(\frac{\partial^2 w}{\partial x \partial \alpha}\right)_i [E_i(\xi_i^2\zeta_i^2) - C_i^2]\\
&\quad + \frac{1}{2}\left(\frac{\partial^2 w}{\partial \alpha^2}\right)_i [E_i(\xi_i\zeta_i^3) - C_i V_i^\alpha] + O(\epsilon^5),\\
\frac{dV_i^\alpha}{dt} &= \frac{1}{2}\left(\frac{\partial^2 w}{\partial x^2}\right)_i [E_i(\xi_i^2\zeta_i^2) - V_i^x V_i^\alpha] + \left(\frac{\partial^2 w}{\partial x \partial \alpha}\right)_i [E_i(\xi_i\zeta_i^3) - C_i V_i^\alpha]\\
&\quad + \frac{1}{2}\left(\frac{\partial^2 w}{\partial \alpha^2}\right)_i [E_i(\zeta_i^4) - (V_i^\alpha)^2] + 2D_\alpha + O(\epsilon^5).
\end{aligned} \tag{42}$$

If we assume that antigenicity and virulence within a morph follow two-dimensional Gaussian distribution for given means, variances and covariance, we should have $E_i(\xi_i^4) = 3(V_i^x)^2, E_i(\xi_i^3\zeta_i) = 3V_i^xC_i,\ E_i(\xi_i^2\zeta_i^2) = V_i^xV_i^\alpha + 2C_i^2,\ E_i(\xi_i\zeta_i^3) = 3V_i^\alpha C_i,$ and $E_i(\zeta_i^4) = 3(V_i^\alpha)^2$, and hence

$$\frac{dV_i^x}{dt} = \left(\frac{\partial^2 w}{\partial x^2}\right)_i (V_i^x)^2 + 2\left(\frac{\partial^2 w}{\partial x \partial \alpha}\right)_i V_i^x C_i + \left(\frac{\partial^2 w}{\partial \alpha^2}\right)_i C_i^2 + 2D_x + O(\epsilon^5), \tag{43}$$

$$\frac{dC_i}{dt} = \left(\frac{\partial^2 w}{\partial x^2}\right)_i V_i^x C_i + \left(\frac{\partial^2 w}{\partial x \partial \alpha}\right)_i \{V_i^x V_i^\alpha - C_i^2\} + \left(\frac{\partial^2 w}{\partial \alpha^2}\right)_i C_i V_i^\alpha + O(\epsilon^5), \tag{44}$$

$$\frac{dV_i^\alpha}{dt} = \left(\frac{\partial^2 w}{\partial x^2}\right)_i C_i^2 + 2\left(\frac{\partial^2 w}{\partial x \partial \alpha}\right)_i V_i^\alpha C_i + \left(\frac{\partial^2 w}{\partial \alpha^2}\right)_i (V_i^\alpha)^2 + 2D_\alpha + O(\epsilon^5), \tag{45}$$

Eqs. (43)-(44) are rewritten in a matrix form as

$$\frac{d\mathbf{G}_i}{dt} = \mathbf{G}_i\mathbf{H}_i\mathbf{G}_i + \begin{pmatrix} 2D_xV_i^x & 0 \\ 0 & 2D_\alpha V_i^\alpha \end{pmatrix} + O(\epsilon^5), \tag{46}$$

where

$$\mathbf{H}_i = \begin{pmatrix} \left(\frac{\partial^2 w}{\partial x^2}\right)_i & \left(\frac{\partial^2 w}{\partial x \partial \alpha}\right)_i \\ \left(\frac{\partial^2 w}{\partial x \partial \alpha}\right)_i & \left(\frac{\partial^2 w}{\partial \alpha^2}\right)_i \end{pmatrix}, \tag{47}$$

is the Hessian of the fitness function of the morph i.

In our case (30) of the joint evolution of antigenicity and virulence of a pathogen after its primary outbreak, the fitness function is given by $w(x,\alpha) = \beta(\alpha)s(x) - \alpha$, and hence $w_i = \beta(\bar{\alpha}_i)s(\bar{x}_i) - \bar{\alpha}_i$, $\left(\frac{\partial w}{\partial x}\right)_i = \beta(\bar{\alpha}_i)s'(\bar{x}_i)$, $\left(\frac{\partial w}{\partial \alpha}\right)_i = \beta'(\bar{\alpha}_i)s(\bar{x}_i) - 1$, $\left(\frac{\partial^2 w}{\partial x^2}\right)_i = \beta(\bar{\alpha}_i)s''(\bar{x}_i)$, $\left(\frac{\partial^2 w}{\partial x \partial \alpha}\right)_i = \beta'(\bar{\alpha}_i)s'(\bar{x}_i)$, $\left(\frac{\partial^2 w}{\partial x \partial \alpha}\right)_i = \beta'(\bar{\alpha}_i)s'(\bar{x}_i)$, and $\left(\frac{\partial^2 w}{\partial \alpha^2}\right)_i = \beta''(\bar{\alpha}_i)s(\bar{x}_i)$, where a prime on $\beta(\alpha)$ and $s(x)$ denotes differentiation by α and x,

562 respectively. Substituting these into the dynamics for morph frequencies (35), for morph
563 means (38)-(39), and for within-morph variance and covariance (43)-(45), we have

$$\frac{dp_i}{dt} = \left[\beta(\bar{\alpha}_i)s(\bar{x}_i) - \bar{\alpha}_i - \sum_j \left(\beta(\bar{\alpha}_j)s(\bar{x}_j) - \bar{\alpha}_j\right)p_j\right]p_i, \tag{48}$$

$$\frac{d\bar{x}_i}{dt} = \beta(\bar{\alpha}_i)s'(\bar{x}_i)V_i^x + \{\beta'(\bar{\alpha}_i)s(\bar{x}_i) - 1\}C_i, \tag{49}$$

$$\frac{d\bar{\alpha}_i}{dt} = \beta(\bar{\alpha}_i)s'(\bar{x}_i)C_i + \{\beta'(\bar{\alpha}_i)s(\bar{x}_i) - 1\}V_i^\alpha, \tag{50}$$

564

$$\frac{dV_i^x}{dt} = \beta(\bar{\alpha}_i)s''(\bar{x}_i)(V_i^x)^2 + 2\beta'(\bar{\alpha}_i)s'(\bar{x}_i)V_i^x C_i + \beta''(\bar{\alpha}_i)s(\bar{x}_i)C_i^2 + 2D_x, \tag{51}$$

$$\frac{dC_i}{dt} = \beta(\bar{\alpha}_i)s''(\bar{x}_i)V_i^x C_i + \beta'(\bar{\alpha}_i)s'(\bar{x}_i)\{V_i^x V_i^\alpha - C_i^2\} + \beta''(\bar{\alpha}_i)s(\bar{x}_i)C_i V_i^\alpha, \tag{52}$$

$$\frac{dV_i^\alpha}{dt} = \beta(\bar{\alpha}_i)s''(\bar{x}_i)C_i^2 + 2\beta'(\bar{\alpha}_i)s'(\bar{x}_i)V_i^\alpha C_i + \beta''(\bar{\alpha}_i)s(\bar{x}_i)(V_i^\alpha)^2 + 2D_\alpha. \tag{53}$$

565 Equations (48)-(53) describe the oligomorphic dynamics of the joint evolution of
566 antigenicity and virulence of a pathogen for a given host susceptibility profile $s(x)$ over
567 pathogen antigenicity.

568 Of particular interest is whether antigenicity or virulence evolve faster when they jointly
569 evolve than when they evolve alone. After the primary outbreak at a given antigenicity, say
570 $x = 0$, the susceptibility $s(x)$ of host population increases due to cross-immunity as the
571 distance $x > 0$ from the antigenicity at the primary outbreak increases. Hence, $s'(\bar{x}_i) >$
572 0. Combining this with the positive tradeoff between transmission rate and virulence, we
573 see that $(\partial^2 w/\partial x \partial \alpha)_i = \beta'(\bar{\alpha}_i)s'(\bar{x}_i) > 0$, and then from (52) we see that the within-
574 morph covariance between antigenicity and virulence becomes positive starting from a zero
575 initial value:

$$\left.\frac{dC_i}{dt}\right|_{C_i=0} = \left(\frac{\partial^2 w}{\partial x \partial \alpha}\right)_i V_i^x V_i^\alpha > 0. \tag{54}$$

If all second moments are sufficiently small initially for an emerging morph, a quick look at the linearization of (51)-(53) around $(V_i^x, C_i, V_i^\alpha) = (0,0,0)$ indicates that both V_i^x and V_i^α become positive due to the random generation of variance by mutation, $D_x > 0$ and $D_\alpha > 0$, while the covariance stays close to zero. Then (54) guarantees that first move of covariance is from zero to positive, which then guarantees that $C_i > 0$ for all t. Therefore, the second term in (38) is positive until the mean virulence reaches its optimum ($\beta'(\alpha)s(x) = 1$). This means that joint evolution with virulence accelerates the evolution of antigenicity. The same is true for virulence evolution: the first term in (39) (which denotes the associated change in virulence due to the selection in antigenicity through genetic covariance between them) is positive, indicating that joint evolution with antigenicity accelerates the virulence evolution.

Numerical example. Fig. 5 shows the oligomorphic dynamics prediction of the emergence of next variant in antigenicity-virulence coevolution. In order to make progress numerically we assume $\mathbf{s}(\mathbf{x})$ to be constant in the following analysis because we are interested in the process between the end of the primary outbreak and the emergence of the next antigenicity virulence morph. The partial differential equations for the density of host $\mathbf{S}(\mathbf{t}, \mathbf{x})$ susceptible to the antigenicity variant $\mathbf{x}$ at time $\mathbf{t}$, and the density of hosts infected by pathogen variant with antigenicity $\mathbf{x}$ and virulence $\boldsymbol{\alpha}$ are

$$\begin{aligned} \frac{\partial S(t,x)}{\partial t} &= -S(t,x)\int_{\alpha_{\min}}^{\alpha_{\max}}\int_0^{x_{\max}} \beta(\alpha)\sigma(x-y)I(t,y,\alpha)\,dy\,d\alpha, \\ \frac{\partial I(t,x,\alpha)}{\partial t} &= [\beta(\alpha)S(t,x) - (\gamma+\alpha)]I(t,x,\alpha) + \left(D_x\frac{\partial^2}{\partial x^2} + D_\alpha\frac{\partial^2}{\partial \alpha^2}\right)I(t,x,\alpha), \end{aligned} \tag{55}$$

with the boundary conditions $(\partial S/\partial x)(t,0) = (\partial S/\partial x)(t,x_{\max}) = 0$, $(\partial I/\partial x)(t,0,\alpha) = (\partial I/\partial x)(t,x_{\max},0) = 0$, $(\partial I/\partial x)(t,x,\alpha_{\min}) = (\partial I/\partial x)(t,x,\alpha_{\max}) = 0$, and the initial conditions $S(0,x) = 1$, and $I(0,x,\alpha) = \epsilon\delta(x)\delta(\alpha)$ where $\delta(\cdot)$ is delta function and $\epsilon = 0.01$. The trait space is restricted in a rectangular region: $0 < x < x_{\max} = 300$ and $\alpha_{\min} = 0.025 < \alpha < 10 = \alpha_{\max}$. Oligomorphic dynamics prediction for the joint evolution of antigenicity and virulence is applied for the next outbreak after the outbreak with the mean antigenicity around $x = 108$ at time $t = 102$. The susceptibility of host to antigenicity variant x at $t_0 = 104.8$ after the previous outbreak peaked around time $t = 102$ came to an end is

$$s(x) = S(t_0, x).$$

This susceptibility profile remains unchanged until the next outbreak starts, and hence the fitness of a pathogen variant with antigenicity x and virulence α is given by

$$w(x,\alpha) = \beta(\alpha)s(x) - (\gamma + \alpha)$$

We bundle the pathogen variants into two morphs at time t_0 at the threshold antigenicity x_c above which the net growth rate of pathogen variant under the given susceptibility profile $s(x)$ and the mean antigenicity becomes positive:

$$w\big(x_c, \bar{\alpha}(t_0)\big) = \beta(\bar{\alpha}(t_0))s(x_c) - \big(\gamma + \bar{\alpha}(t_0)\big) = 0.$$

The initial frequency and the moments of two morphs, the variant 0 with $x < x_c$ and the variant 1 with $x > x_c$ are then calculated respectively from the joint distribution $I(t_0, x, \alpha)$ in the restricted region $\{(x,\alpha); 0 < x < x_c, \alpha_{\min} < \alpha < \alpha_{\max}\}$ and that in the restricted region $\{(x,\alpha);\ x_c < x < x_{\max}, \alpha_{\min} < \alpha < \alpha_{\max}\}$. The frequency p_1 of the morph 1 (the frequency of the morph 0 is given by $p_0 = 1 - p_1$), the mean antigenicity $\bar{x}_i$ and mean

618 virulence $\bar{\alpha}_i$ of the morph i, and variances and covariance, V_i^x, C_i, V_i^α of the morph i ($i =$
619 0,1) follow (48)-(53), where the dynamics for the morph frequency (48) is simplified in
620 this two morph situation as

621 $$\frac{dp_1}{dt} = [\beta(\bar{\alpha}_1)s(\bar{x}_1) - \beta(\bar{\alpha}_0)s(\bar{x}_0) - (\bar{\alpha}_1 - \bar{\alpha}_0)]p_1(1 - p_1),$$

622 with $p_0(t) = 1 - p_1(t)$. This is iterated from $t = t_0 = 104.8$ to $t_e = 107$. The frequency
623 $p_1$of the new morph, the population mean antigenicity $\bar{x} = p_0\bar{x}_0 + p_1\bar{x}_1$, virulence $\bar{\alpha} =$
624 $p_0\bar{\alpha}_0 + p_1\bar{\alpha}_1$, variance in antigenicity $V_x = p_0V_0^x + p_1V_1^x$, covariance between antigenicity
625 and virulence $C = p_0C_0 + p_1C_1$, and variance in virulence $V_\alpha = p_0V_0^\alpha + p_1V_1^\alpha$ are
626 overlayed by red thick curves on the trajectories of moments observed in full dynamics
627 (55).

628 In the panel (a) of Fig. 5, the dashed vertical line represents the threshold antigenicity x_c
629 above which $R_0 = \beta s(x)/(\gamma + \bar{\alpha}) > 1$ at $t = t_s = 104.8$ where oligomorphic dynamics
630 (OMD) prediction is attempted. Two morphs are then defined according to whether or not
631 the antigenicity exceeds a threshold $x = x_c$: the resident morph (morph 1) is represented
632 as the dense cloud to the left of $x = x_c$ and the second morph (morph 2) consisting of all
633 the genotypes to the right of $x = x_c$ with their R_0 greater than one. The within-morph
634 means and variances are then calculated in each region. The relative total densities of
635 infected hosts in the left and right regions defines the initial frequency of two morphs in
636 OMD. A 2D Gaussian distribution is assumed for within-morph trait distributions to have
637 the closed moment equations as explained before. Using these as the initial means,
638 variances, covariances of the two morphs at $t = t_s$, the oligomorphic dynamics for 11
639 variables (relative frequency of morph 1, mean antigenicity, mean virulence, variances in

antigenicity and virulence and their covariance in morph 0 and 1) is integrated up to $t = t_e$. The results are shown in red curves in the panels of second and third rows, which are compared with the simulation results (blue curves).

The panels (c)-(e) in Fig. 5 show the change in total infected density (c), mean antigenicity (d), and mean virulence (e). Red curves show the prediction by oligomorphic dynamics from the initial moments of each morph at $t = t_s$ to the susceptibility distribution $s(x) = S(t_s, x)$. Red curves in the (e) and (e) show the OMD prediction, which is compared with the simulation results (blue curves). The OMD predicted mean antigenicity, for example, is defined as

$$\bar{x}(t) = \big(1 - p_1(t)\big)\bar{x}_0(t) + p_1(t)\bar{x}_1(t),$$

where $p_1(t)$ is the frequency of morph 1, $\bar{x}_0$ and $\bar{x}_1$ are the mean antigenicity of morph 0 and 1.

The red curves in the third row (f)-(h) of Fig. 5 show the OMD-predicted changes in the variance in antigenicity, variance in virulence, and covariance between antigenicity and virulence, which are compared with the simulation results (blue curves). The OMD predicted covariance, for example, is defined as

$$C(t) = (1 - p_1(t))C_0(t) + p_1(t)C_1(t) + p_1(t)\big(1 - p_1(t)\big)\big(\bar{x}_0(t) - \bar{x}_1(t)\big)\big(\bar{\alpha}_0(t) - \bar{\alpha}_1(t)\big)$$

where $C_0(t)$ and $C_1(t)$ are antigenicity-virulence covariance in morph 0 and 1, and $\bar{\alpha}_0(t)$ and $\bar{\alpha}_1(t)$ are mean virulence of morph 0 and 1.

Selection for maximum growth rate

We next show that a pathogen that has the strategy maximizing the growth rate in a fully susceptible population is evolutionarily stable in the presence of antigenic escape.

At stationarity, the travelling wave profiles of $\hat{I}(z)$ and $\hat{S}(z)$ along the moving coordinate, $z = x - vt$, that drifts constantly to right with the speed v are defined as

$$\begin{aligned} 0 &= D\frac{d^2\hat{I}(z)}{dz^2} + v\frac{d\hat{I}(z)}{dz} + \beta\hat{S}(z)\hat{I}(z) - (\gamma+\alpha)\hat{I}(z), \\ 0 &= v\frac{d\hat{S}(z)}{dz} - \beta\hat{S}(z)\int_{-\infty}^{\infty}\sigma(z-\xi)\hat{I}(\xi)\,d\xi. \end{aligned} \tag{56}$$

with $\hat{I}(-\infty) = \hat{I}(\infty) = 0, \hat{S}(\infty) = 1$.

Let $j(t,x)$ be the density of a mutant pathogen variant with virulence α' and transmission rate β' that is introduced in the host population where the resident variant is already established (50). For the initial transient phase in which the density of mutant is sufficiently small, we have an equation for the change in $J(t,z) = j(t,x)$:

$$\frac{\partial}{\partial t}J(t,z) = \left\{D\frac{\partial^2}{\partial z^2} + v\frac{\partial}{\partial z} + \beta'\hat{S}(z) - (\gamma+\alpha')\right\}J(t,z), \tag{57}$$

with the initial condition $J(0,z) = \epsilon\delta(z)$, where ϵ is a small constant and $\delta(\cdot)$ is Dirac function.

Consider a system

$$\frac{\partial w}{\partial t} = \left\{D\frac{\partial^2}{\partial z^2} + v\frac{\partial}{\partial z} + \beta' - (\gamma+\alpha')\right\}w, \tag{58}$$

677 with $w(0,z) = J(0,z) = \epsilon\delta(z)$. Noting that $\hat{S}(z) < 1$, we have $J(t,z) \leq w(t,z)$ for any

678 $t > 0$ and $z \in \mathbb{R}$ from the comparison theorem. The solution to (52) is

679 $$w(t,z) = \frac{\epsilon}{\sqrt{4\pi Dt}} \exp\left[r't - \frac{(z+vt)^2}{4Dt}\right] \tag{59}$$

680 where $r' = \beta' - (\gamma + \alpha')$. This follows by noting that $w(t,x)e^{-r't}$ follows a simple

681 diffusion equation $\partial w/\partial t = D\partial^2 w/\partial x^2$. By rearranging the exponents of (53),

682 $$\begin{aligned} w(t,z) &= \exp[at - kz] \frac{\epsilon}{\sqrt{4\pi Dt}} e^{-z^2/4Dt} \\ &< \frac{\epsilon}{\sqrt{4\pi Dt}} \exp[at - kz] \end{aligned} \tag{60}$$

683 where

684 $$a = \frac{v'^2 - v^2}{4D}, \tag{61}$$

$$k = \frac{v}{2D}. \tag{62}$$

685 Here $v' = 2\sqrt{r'D}$ is the asymptotic wave speed if the mutant variant monopolizes the host

686 population. Therefore, if $v' < v$, then $a < 0$, and hence $w(t,z)$ for a fixed z converges to

687 zero as t goes to infinity; which in turn implies that $J(t,z)$ converges to zero because

688 $J(t,z) \leq w(t,z)$ for all t and z. Therefore, we conclude that any mutant that has a slower

689 wave speed than the resident can never invade the population, implying that a variant that

690 has the maximum wave speed $v = 2\sqrt{rD}$ is locally evolutionarily stable.

691 **Figure Legends**

692 **Fig. 1: Continuous antigenic drift (a) and periodical antigenic shifts (b) of the model**.
693 The grey colored surface denotes the infected density $I(t,x)$ varying in time t and
694 antigenicty x, and the yellow colored surface denotes the density of hosts $S(t,x)$ that are
695 susceptible to antigenicity variant x of pathogen at time t. The cross immunity $\sigma(x) =$
696 $\exp(-x^2/2\omega^2)$ has a width of $\omega = 0.2$ in (a) and $\omega = 0.6$ in (b). Other parameters are
697 $\beta = 2,\ \alpha = 0.1,\ \gamma = 0.5,$ and $D = 0.001$.

698

699 **Fig. 2: Oligomorphic dynamics prediction of the emergence of antigenicity shift.** (a)
700 Oligomorphic prediction for the change in the mean antigenicity after the primary outbreak
701 at $x = 0$ and that after the second outbreak starting around $x = 5.5$ (red curves), compared
702 with that obtained by numerical simulations (blue dots). (b) Heat map representation of
703 the time change of the antigenic drift model (1). Parameters: $\beta = 2, \gamma + \alpha = 0.6, \sigma(x) =$
704 $\exp(-x^2/2\omega^2)$ with $\omega = 2$, $D = 0.001$. Initially, all hosts are equally susceptible with
705 $S(0,x) = 1$. The primary pathogen variant is introduced at $x = 0$ with infected density
706 0.001.

707

708 **Fig. 3: Marginal distribution of antigenicity (left) and virulence (right) in the absence**
709 **(a) or presence (b) of cross-immunity**. (a) No cross immunity is assumed so that each
710 antigenicity genotype causes specific herd immunity: $\sigma(x-y) = \delta(x-y)$, where $\delta(\cdot)$ is
711 Dirac's delta function. There are 1600 antigenic variations having equally divided
712 antigenicity between 0 and 80. (b) We assume a Gaussian cross-immunity kernel,

713 $\sigma(x-y) = \exp(-(x-y)^2/2\omega^2)$, with width $\omega = 5$. There are 300 antigenic variations
714 having equally divided antigenicity between 0 and 300. In both panels, there are 100 viral
715 virulence traits each having virulence equally divided between 0 and 20, and Diffusion
716 constants due to mutations are $D_x = 0.01$ (for antigenicity) and $D_\alpha = 0.01$(for virulence).
717 The blue dashed lines show the ES virulence predicted from maximizing R0, as expected
718 in the absence of antigenic escape, while the red dashed lines show the predicted ES
719 virulence that maximizes $r(\alpha) = \beta(\alpha) - (\gamma + \alpha)$ as predicted from our analysis. Other
720 parameters: $\gamma = 0.5$, and $\beta(\alpha) = 5\sqrt{\alpha}$.

721

722 **Fig. 4: Graphical representation of the predicted ES virulence with or without**
723 **antigenic escape under the assumption of a transmission-virulence trade-off.** In the
724 absence of antigenic escape, the ES virulence, α_R^*, can be predicted from the maximization
725 of the pathogen's epidemiological basic reproduction ratio, $R_0 = \beta/(\gamma + \alpha)$, or
726 equivalently by the minimization of the total density of susceptible hosts since, at
727 equilibrium, $s^* = 1/R_0$. The slope of the transmission-virulence trade-off at the ESS is
728 then $1/s^* = R_0$. With antigenic escape, the ES virulence, α_r^*, can be predicted from the
729 maximization of the pathogen's growth rate in a fully susceptible population, $r_0 = \beta(\alpha) -$
730 $(\gamma + \alpha)$. The slope of the transmission-virulence trade-off at the ESS is then 1. This holds
731 true in the limit of a large antigenicity trait, but intermediate values of ES virulence,
732 corresponding to intermediate slopes, can also be selected for if other processes constrain
733 the evolution of the antigenicity trait, as explained in the main text.

734

Fig. 5: Oligomorphic dynamics predictions compared to the simulation results of the emergence of the next variant during antigenicity-virulence coevolution. Panels (a) and (b) are simulation results showing snapshots of contour plots for the joint trait distribution observed near (a) the starting and (b) finishing time of emergence. The overlaid curves are the trajectory of mean traits $(\bar{x}, \bar{\alpha})$ up $t = 104.8$ and $t = 109$ observed in the simulation. Panels (c)-(h) show the dynamics of the total density of infected hosts, mean antigenicity, mean virulence, the variance in antigenicity, the variance in virulence, and the covariance between antigenicity and virulence, respectively predicted by the oligomorphic analysis compared to the simulation results. Parameters: $\gamma = 0.5$, $\beta(\alpha) = 5\sqrt{\alpha}$, $D_x = 0.005$, $D_\alpha = 0.0002$. As in Fig. 2 we assume a Gaussian cross-immunity kernel, $\sigma(x - y) = \exp(-(x - y)^2/2\omega^2)$, with width $\omega = 5$. The oligomorphic dynamics describing the changes in the frequency $p_0(t) = 1 - p_1(t)$ of the currently prevailing morph at time $t_s = 104.8$ and the frequency $p_1(t)$ of upcoming morph, the mean antigenicity $\bar{x}_i(t)$ and mean virulence $\bar{\alpha}_i(t)$ of the two morphs $(i = 0,1)$, and the within-morph variances V_i^x and V_i^α in antigenicity and virulence, as well as the within-morph covariance $C_i(t)$ between antigenicity and virulence in each morph $(i = 0,1)$ are defined as (48)-(53) in the methods.

Acknowledgements: This study was supported by grants from the NIH R01 GM122061-03 and the NSF DEB- 2011109 to MB, ANR JCJC grant ANR-16-CE35-0012-01 to SL and the ESB Cooperation Program, The Graduate University for Advanced Studies, SOKENDAI to AS.

Author contributions: MB, AS and SL contributed to the conception of the project, the writing of the original draft, editing and revision of the paper. AS and SL carried out the analysis of the model.

Code Availability:

All code is available at https://github.com/MikeBoots/AntigenicEscape

Competing interests:

The authors declare no competing interests

References

1. Fauci, A. S. & Morens, D. M. Zika virus in the Americas—yet another arbovirus threat. *New England Journal of Medicine* **374**, 601–604 (2016).
2. Organization, W. H. Coronavirus disease 2019 (COVID-19): situation report, 72. (2020).
3. Remuzzi, A. & Remuzzi, G. COVID-19 and Italy: what next? *The Lancet* (2020).
4. Keeling, M. J. *et al*. Dynamics of the 2001 UK foot and mouth epidemic: Stochastic dispersal in a heterogeneous landscape. *Science* **294**, 813–817 (2001).
5. Hudson, P., Dobson, A. & Newborn, D. Prevention of population cycles by parasite removal. *Science* **282**, 2256 (1998).
6. Dobson, A. P. & May, R. M. DISEASE AND CONSERVATION. in *Soule, M. E.* 345–366 (1986).

7. Anderson, R. M. & May, R. M. *Infectious Diseases of Humans*. (Oxford University Press, 1991).

8. May, R. M. & Anderson, R. M. Parasite Host Coevolution. *Parasitology* **100**, S89–S101 (1990).

9. Bremermann, H. J. & Pickering, J. A Game-Theoretical Model of Parasite Virulence. *J. Theor. Biol.* **100**, 411–426 (1983).

10. Alizon, S., Hurford, A., Mideo, N. & Van Baalen, M. Virulence evolution and the trade-off hypothesis: history, current state of affairs and the future. *Journal of Evolutionary Biology* **22**, 245–259 (2009).

11. Bremermann, H. J. & Thieme, H. R. A Competitive-Exclusion Principle for Pathogen Virulence. *J. Math. Biol.* **27**, 179–190 (1989).

12. Alizon, S., de Roode, J. C. & Michalakis, Y. Multiple infections and the evolution of virulence. *Ecology Letters* **16**, 556–567 (2013).

13. Lion, S. & Boots, M. Are parasites ‘“prudent”’ in space? *Ecology letters* **13**, 1245–1255 (2010).

14. van Baalen, M. Coevolution of recovery ability and virulence. *Proceedings of the Royal Society of London Series B-Biological Sciences* **265**, 317–325 (1998).

15. Lion, S. & Metz, J. A. Beyond R0 maximisation: on pathogen evolution and environmental dimensions. *Trends in ecology & evolution* **33**, 458–473 (2018).

16. Day, T. & Gandon, S. Applying population-genetic models in theoretical evolutionary epidemiology. *Ecology Letters* **10**, 876–888 (2007).

17. Day, T. & Proulx, S. R. A general theory for the evolutionary dynamics of virulence. *Am. Nat.* **163**, E40–E63 (2004).

18. Frank, S. A. Ecological and Genetic Models of Host Pathogen Coevolution. *Heredity* **67**, 73–83 (1991).

19. Lenski, R. E. & May, R. M. The Evolution of Virulence in Parasites and Pathogens - Reconciliation between 2 Competing Hypotheses. *J. Theor. Biol.* **169**, 253–265 (1994).

20. Archetti, I. & Horsfall Jr, F. L. Persistent antigenic variation of influenza A viruses after incomplete neutralization in ovo with heterologous immune serum. *The Journal of experimental medicine* **92**, 441–462 (1950).

21. Smith, D. J. *et al*. Mapping the antigenic and genetic evolution of influenza virus. *science* **305**, 371–376 (2004).

22. Hensley, S. E. *et al*. Hemagglutinin receptor binding avidity drives influenza A virus antigenic drift. *Science* **326**, 734–736 (2009).

23. Gupta, S. *et al*. The maintenance of strain structure in populations of recombining infectious agents. *Nat. Med.* **2**, 437–442 (1996).

24. Haraguchi, Y. & Sasaki, A. Evolutionary pattern of intra-host pathogen antigenic drift: Effect of cross-reactivity in immune response. *Philos. Trans. R. Soc. Lond. Ser. B-Biol. Sci.* **352**, 11–20 (1997).

25. Sasaki, A. & Haraguchi, Y. Antigenic drift of viruses within a host: A finite site model with demographic stochasticity. *J. Mol. Evol.* **51**, 245–255 (2000).

26. Gog, J. R. & Grenfell, B. T. Dynamics and selection of many-strain pathogens. *Proc. Natl. Acad. Sci. U. S. A.* **99**, 17209–17214 (2002).

27. Anderson, R. M. & May, R. M. Coevolution of Hosts and Parasites. *Parasitology* **85**, 411–426 (1982).

28. Sasaki, A. & Dieckmann, U. Oligomorphic dynamics for analyzing the quantitative genetics of adaptive speciation. *Journal of Mathematical Biology* **63**, 601–635 (2011).
29. Kimura, M. A stochastic model concerning the maintenance of genetic variability in quantitative characters.
30. LANDE, R. MAINTENANCE OF GENETIC-VARIABILITY BY MUTATION IN A POLYGENIC CHARACTER WITH LINKED LOCI. *GENETICAL RESEARCH* **26**, 221–235 (1975).
31. Sasaki, A. Evolution of antigen drift/switching - continuously evading pathogens. *Journal of Theoretical Biology* **168**, 291–308 (1994).
32. Haraguchi, Y. & Sasaki, A. Evolutionary pattern of intra–host pathogen antigenic drift: effect of cross–reactivity in immune response. *Philosophical Transactions of the Royal Society of London. Series B: Biological Sciences* **352**, 11–20 (1997).
33. Bull, J. J. & Ebert, D. Invasion thresholds and the evolution of nonequilibrium virulence. *Evolutionary Applications* **1**, 172–182 (2008).
34. Matsuzaki, Y. *et al*. Neutralizing epitopes and residues mediating the potential antigenic drift of the hemagglutinin-esterase protein of influenza C virus. *Viruses* **10**, 417 (2018).
35. Zambon, M. C. Epidemiology and pathogenesis of influenza. *Journal of Antimicrobial Chemotherapy* **44**, 3–9 (1999).
36. Yamashita, M., Krystal, M., Fitch, W. M. & Palese, P. Influenza B virus evolution: co-circulating lineages and comparison of evolutionary pattern with those of influenza A and C viruses. *Virology* **163**, 112–122 (1988).

37. Medina, R. A. & García-Sastre, A. Influenza A viruses: new research developments. *Nature Reviews Microbiology* **9**, 590–603 (2011).

38. Fedson, D. S. Pandemic influenza and the global vaccine supply. *Clinical infectious diseases* **36**, 1552–1561 (2003).

39. Subramanian, R., Graham, A. L., Grenfell, B. T. & Arinaminpathy, N. Universal or specific? A modeling-based comparison of broad-spectrum influenza vaccines against conventional, strain-matched vaccines. *PLoS computational biology* **12**, e1005204 (2016).

40. Christiansen, F. B. ON CONDITIONS FOR EVOLUTIONARY STABILITY FOR A CONTINUOUSLY VARYING CHARACTER. *American Naturalist* **138**, 37–50 (1991).

41. Geritz, S. A. H., van der Meijden, E. & Metz, J. A. J. Evolutionary dynamics of seed size and seedling competitive ability. *Theor. Popul. Biol.* **55**, 324–343 (1999).

42. LANDE, R. QUANTITATIVE GENETIC-ANALYSIS OF MULTIVARIATE EVOLUTION, APPLIED TO BRAIN - BODY SIZE ALLOMETRY. *EVOLUTION* **33**, 402–416 (1979).

43. LANDE, R. MODELS OF SPECIATION BY SEXUAL SELECTION ON POLYGENIC TRAITS. *PROCEEDINGS OF THE NATIONAL ACADEMY OF SCIENCES OF THE UNITED STATES OF AMERICA-BIOLOGICAL SCIENCES* **78**, 3721–3725 (1981).

44. Boots, M., White, A., Best, A. & Bowers, R. HOW SPECIFICITY AND EPIDEMIOLOGY DRIVE THE COEVOLUTION OF STATIC TRAIT DIVERSITY IN HOSTS AND PARASITES. *Evolution* **68**, 1594–1606 (2014).

45. Koelle, K., Cobey, S., Grenfell, B. & Pascual, M. Epochal Evolution Shapes the Phylodynamics of Interpandemic Influenza A (H3N2) in Humans. *Science* **314**, 1898 (2006).

46. Bedford, T. *et al*. Global circulation patterns of seasonal influenza viruses vary with antigenic drift. *Nature* **523**, 217 (2015).

47. Bedford, T., Rambaut, A. & Pascual, M. Canalization of the evolutionary trajectory of the human influenza virus. *BMC biology* **10**, 1–12 (2012).

48. Zinder, D., Bedford, T., Gupta, S. & Pascual, M. The roles of competition and mutation in shaping antigenic and genetic diversity in influenza. *PLoS Pathog* **9**, e1003104 (2013).

49. Eguia, R. *et al*. A human coronavirus evolves antigenically to escape antibody immunity. *bioRxiv* 2020.12.17.423313 (2020) doi:10.1101/2020.12.17.423313.

50. Gandon, S., Mackinnon, M. J., Nee, S. & Read, A. F. Imperfect vaccines and the evolution of pathogen virulence. *Nature* **414**, 751–756 (2001).

51. Read, A.F. *et al*. Imperfect vaccination can enhance the transmission of highly virulent pathogens. *PloS Biol* **13**, e1002198.

52. Day, T., Gandon, S., Lion, S. & Otto, S. P. On the evolutionary epidemiology of SARS-CoV-2. *Current Biology* **30**, R849–R857 (2020).

53. Visher, E. *et al*. *The Three Ts of Pathogen Evolution During Zoonotic Emergence*. https://osf.io/tueyb (2021) doi:10.32942/osf.io/tueyb.

54. Chesson, P. Mechanisms of maintenance of species diversity. *Annual review of Ecology and Systematics* **31**, 343–366 (2000).

893

Fig. 1: Sasaki, Lion, Boots

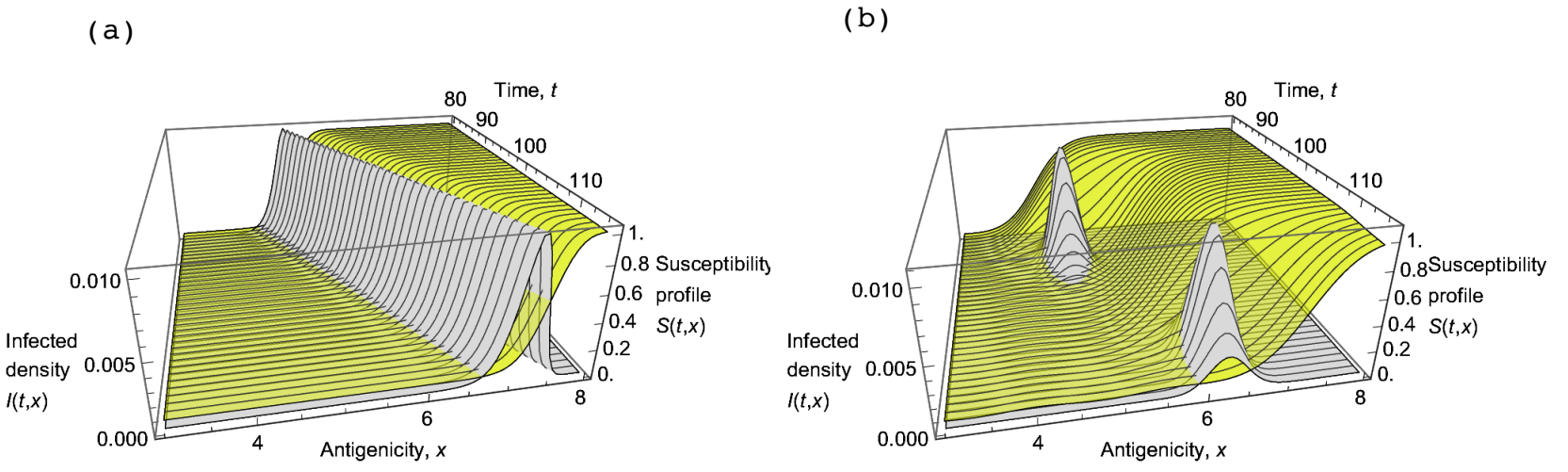

Fig. 2: Sasaki, Lion, Boots

(a)

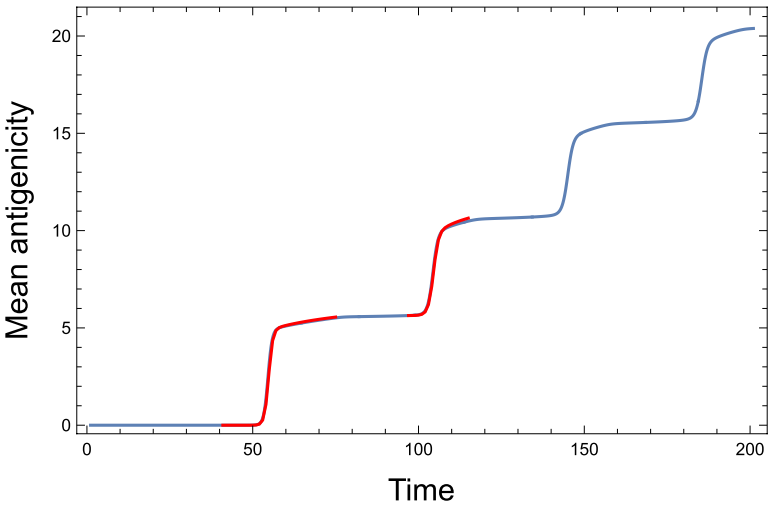

(b)

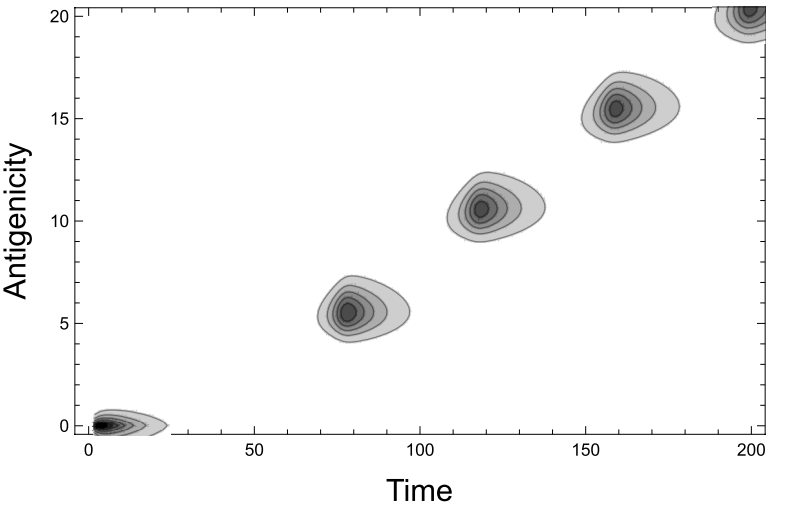

(a) Without cross-immunity

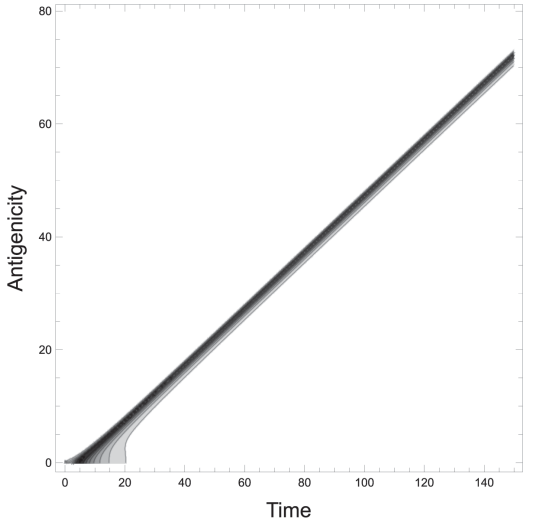

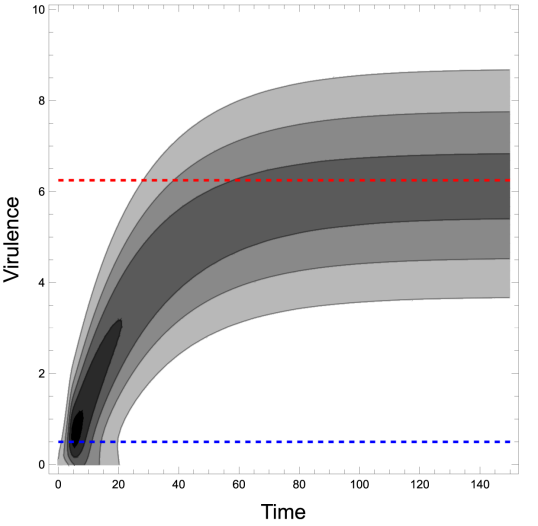

(b) With cross-immunity

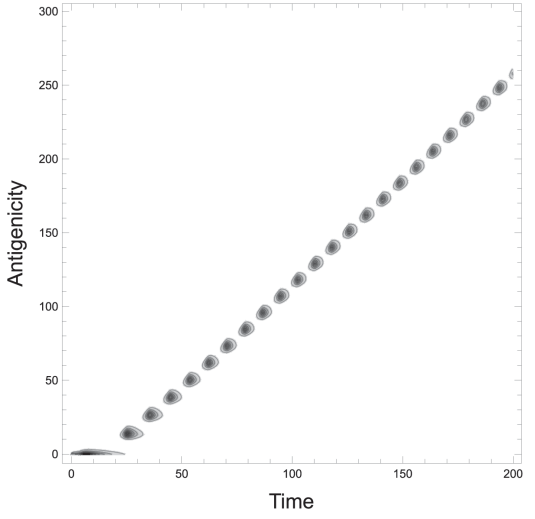

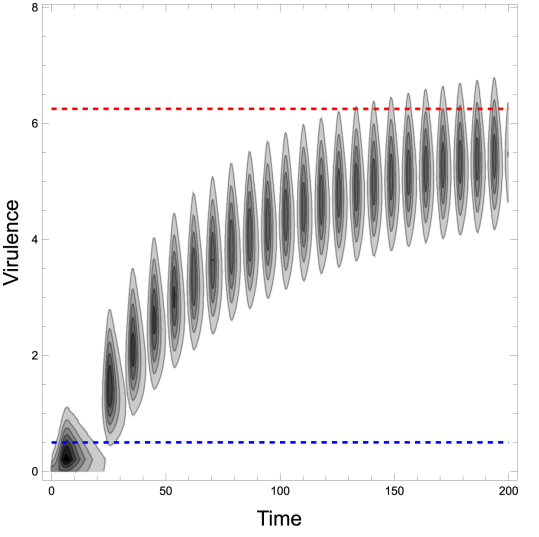

Fig. 4. Sasaki, Lion, Boots

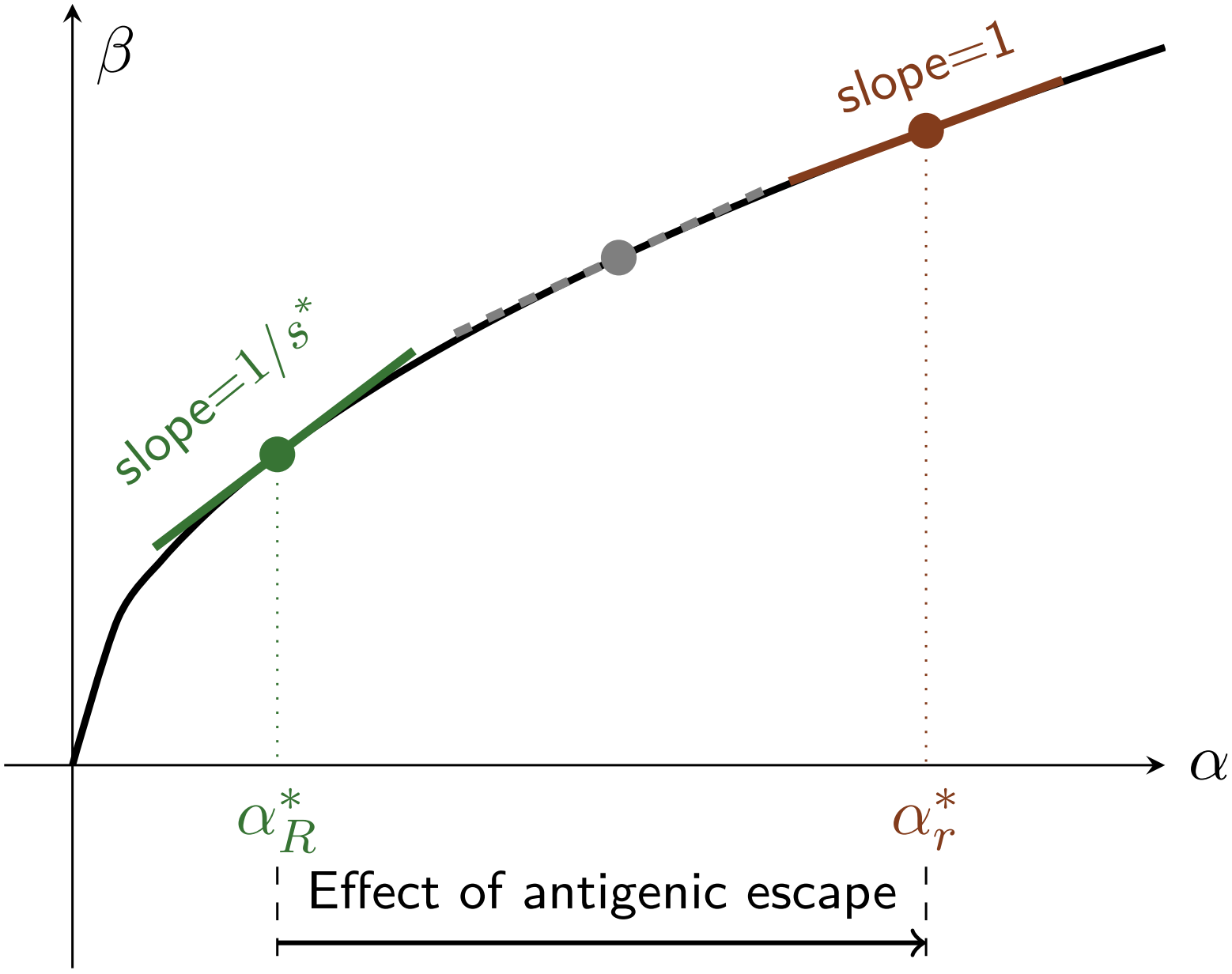

Fig. 5: Sasaki, Lion, Boots

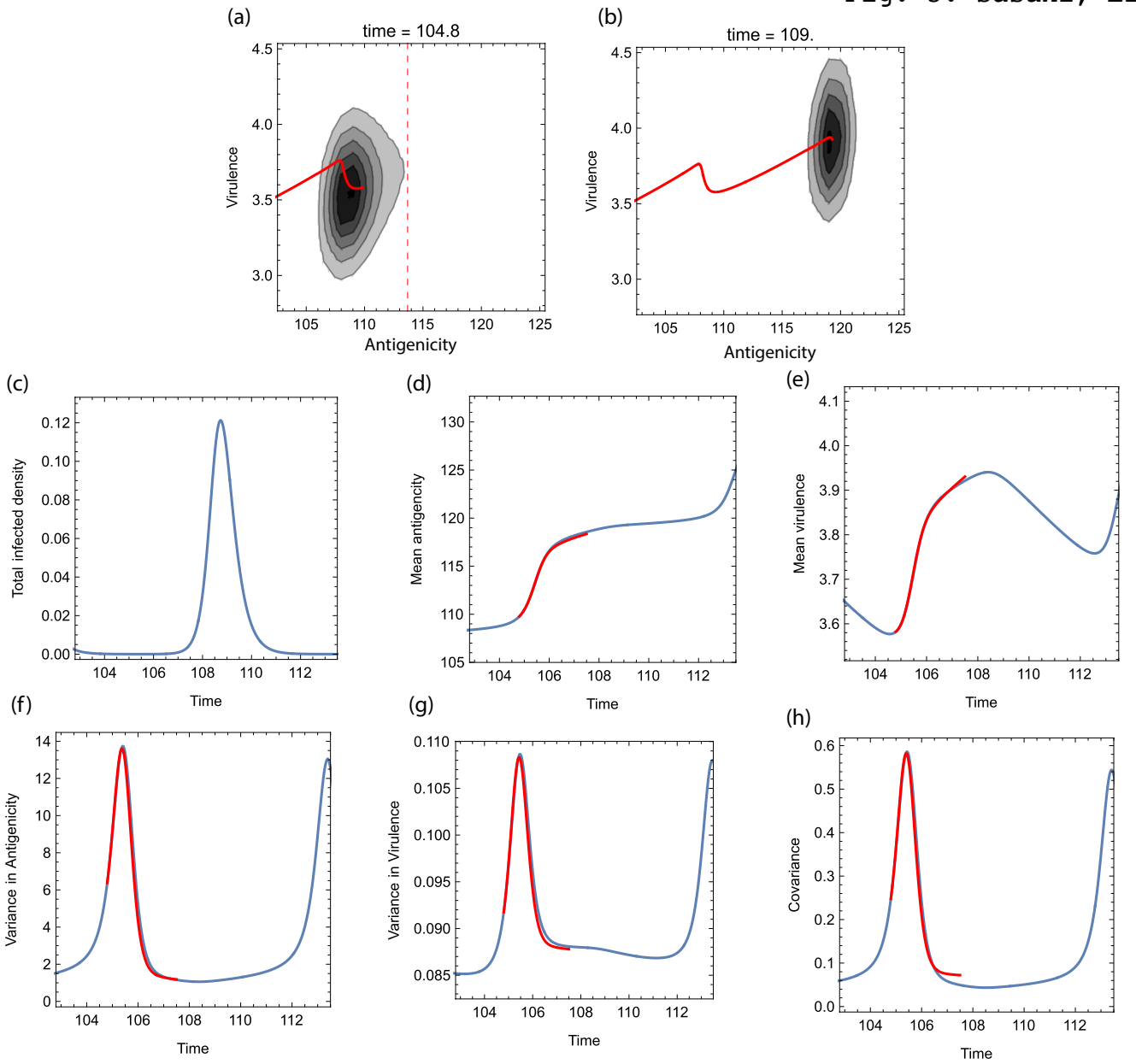

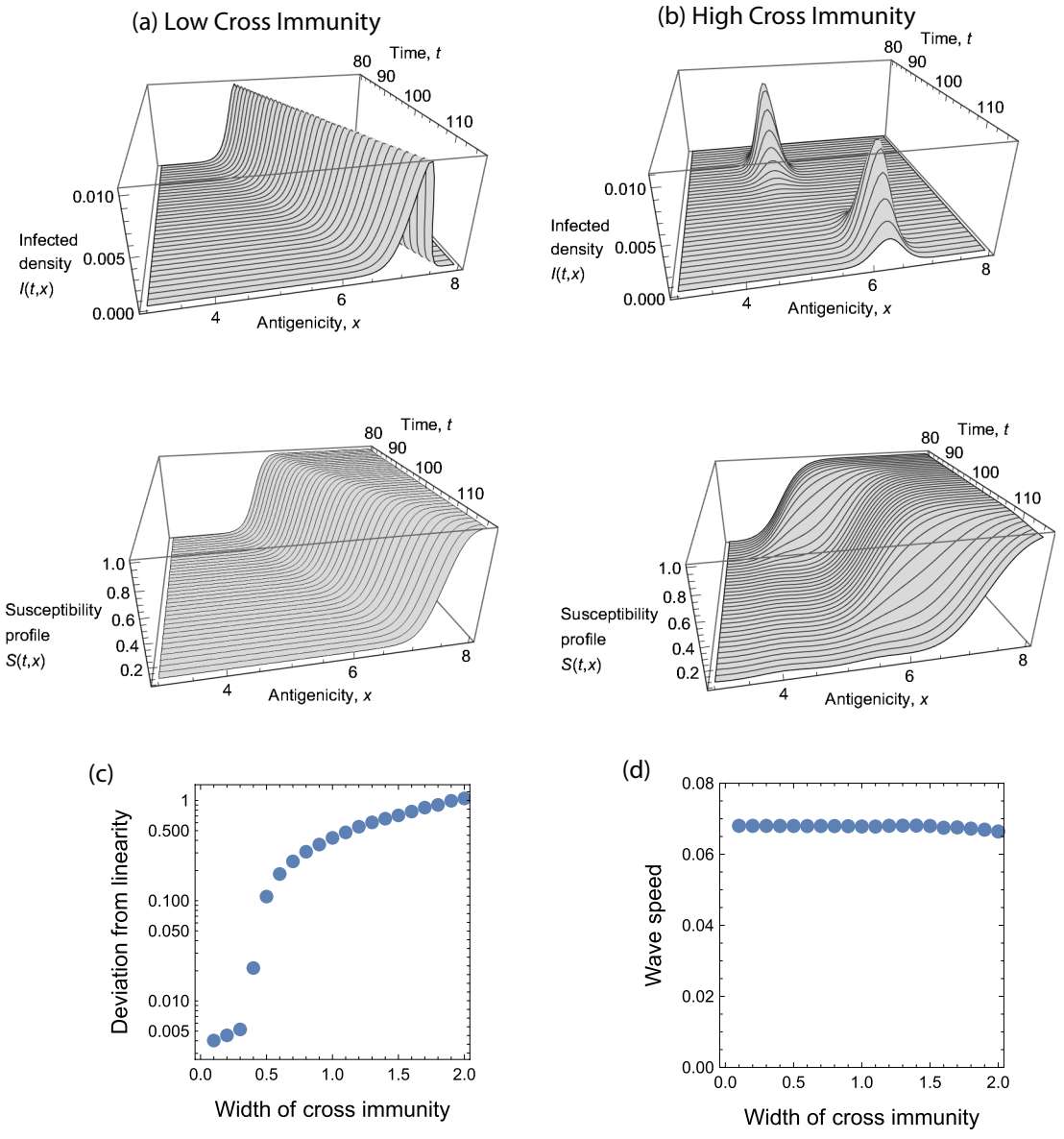
(a) Low Cross Immunity
(b) High Cross Immunity
Time, t
80
90
100
110
Infected density I(t,x)
0.010
0.005
0.000
Antigenicity, x
4
6
8
Susceptibility profile S(t,x)
1.0
0.8
0.6
0.4
0.2
(c)
Deviation from linearity
1
0.500
0.100
0.050
0.010
0.005
0.0
0.5
1.0
1.5
2.0
Width of cross immunity
(d)
Wave speed
0.08
0.06
0.04
0.02
0.00

Ext Fig. 2: Sasaki, Lion, Boots

(a)

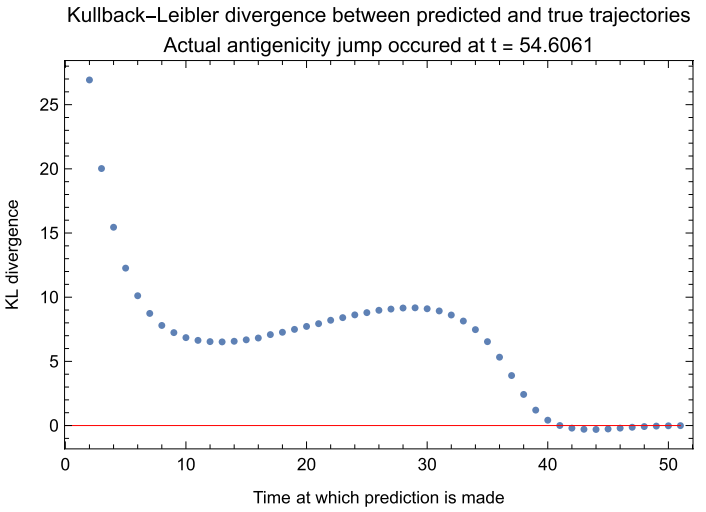

(b)

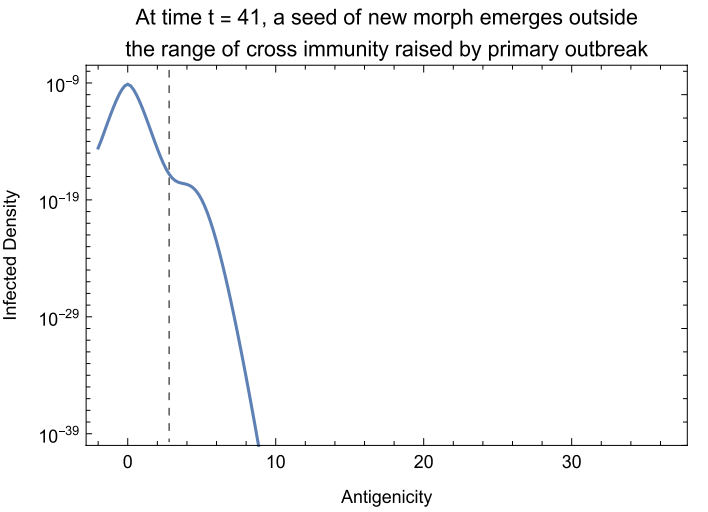

Supplementary Information: Sasaki, Lion and Boots – "Antigenic escape selects for the evolution of higher virulence"

Multidimensional antigenic space

Here we show that our key results obtained with using 1-dimensional antigenic space remain the same when we extend the antigenicity space into two dimensions. We first describe our antigenic drift model in 2-dimensional space. Let $S(t,\mathrm{x})$ be the density of hosts that are susceptible to pathogens of antigenicity $\mathrm{x}=(x_1,x_2)$= at time t. Let also $I(t,\mathrm{x},\alpha)$ be the density of hosts that are currently infected and infectious with the pathogen of antigenicity x and virulence α at time t. These distributions change with time as

$$\frac{\partial S(t,\mathrm{x})}{\partial t} = -S(t,\mathrm{x})\int_{-\infty}^{\infty}\int_{-\infty}^{\infty}\int_{0}^{\infty}\beta(\alpha)\sigma(\mathrm{x}-\mathrm{y})I(t,\mathrm{y},\alpha)\,d\alpha\,dy_1dy_2,$$
$$\frac{\partial I(t,\mathrm{x},\alpha)}{\partial t} = [\beta(\alpha)S(t,\mathrm{x})-(\gamma+\alpha)]I(t,\mathrm{x},\alpha)+D\nabla_{\mathbf{x}}^2 I + D_\alpha\frac{\partial^2 I}{\partial\alpha^2},$$

where γ is recovery rate, α is virulence, $\beta(\alpha)$ is transmission rate as a function of virulence,

$$\sigma(|\mathrm{x}-\mathrm{y}|)=\exp\left[-\frac{|\mathrm{x}-\mathrm{y}|^2}{2\omega^2}\right]$$

denotes the degree of cross-immunity between viruses of antigenicity x and y, where $|\mathrm{x}-\mathrm{y}|=\sqrt{(x_1-y_1)^2+(x_2-y_2)^2}$ is antigenic distance between them, $\nabla_{\mathbf{x}}^2=\frac{\partial^2}{\partial x_1^2}+\frac{\partial^2}{\partial x_2^2}$, $D=\frac{1}{2}\mu m^2$ is the half of mutation variance for the changes in antigenicity (the mutation is assumed to be isotropic in either direction in 2-dimensional antigenic space), $D_\alpha=\mu_\alpha m_\alpha^2$ is the half of mutation variance for the change in virulence. The initial host population is assumed to be susceptible to any antigenicity variant of pathogen: $S(0,\mathrm{x})=1$, for all x.

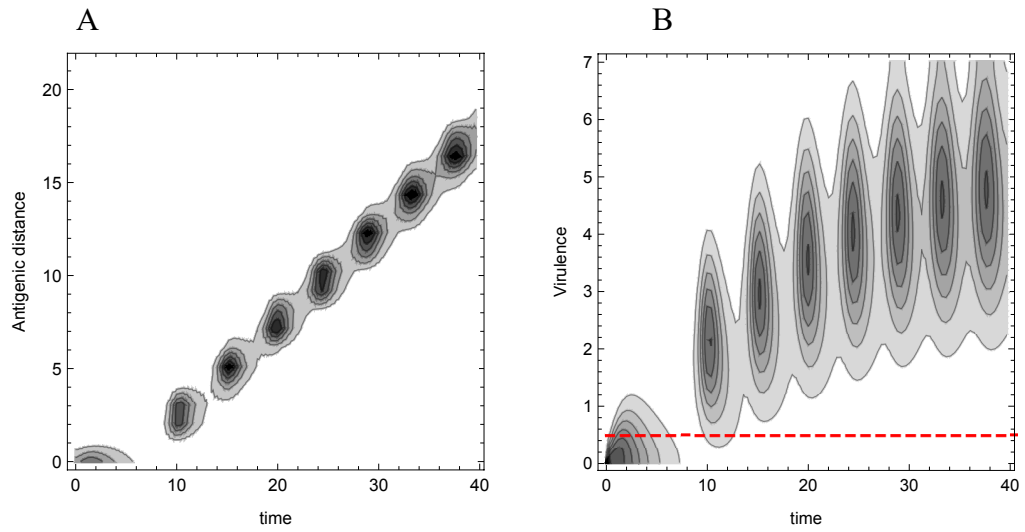

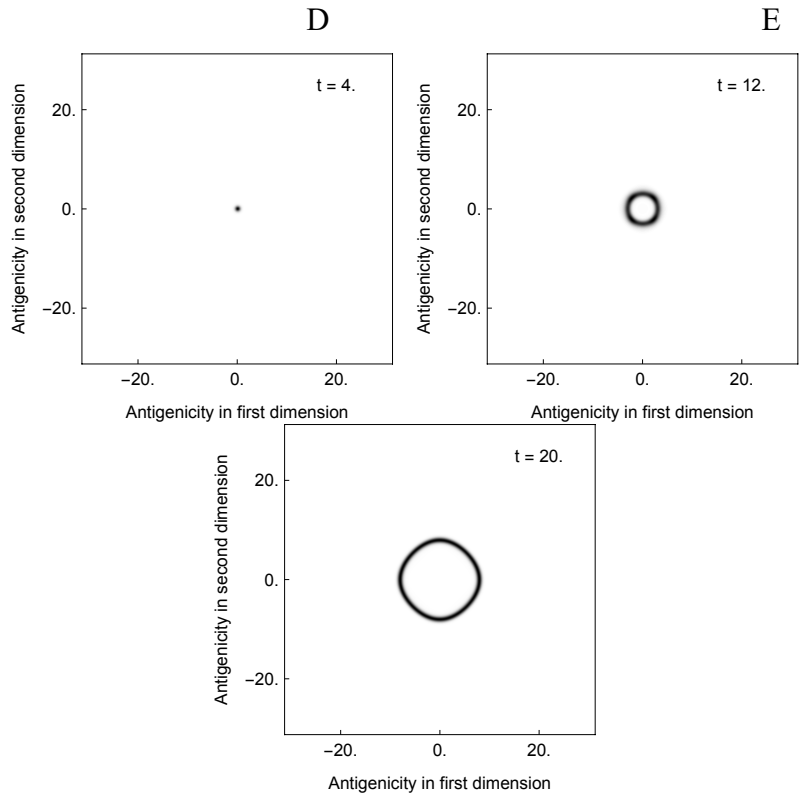

Supplementary Figure 1, Joint evolution of virulence and antigenicity in 2-dimensional antigenic space. A) The time change in the distribution of antigenic distance, $r = \sqrt{x_1^2 + x_2^2}$, of viruses from their founder variant at antigenicity $(x_1, x_2) = (0,0)$ and time $t = 0$. B) The time change in the virulencefrom its initial value $\alpha = 0.025$ at time $t = 0$. The dashed line at $\alpha = 0.5$ indicates the ESS virulence in the endemic population which

should have been attained if there were no antigenic escape. C-E) The snapshots of the 2-dimensional antigenicity distribution at time $t = 4$, 12 and 20. See Equation (S.1) for the model. The transmission rate β and virulence α has a tradeoff $\beta = 5\sqrt{\alpha}$. The recovery rate is $\gamma = 0.5$. The partial cross-immunity between two virus variants with antigenic distance r is $\sigma(r) = \exp(-r^2/2\omega^2)$, where the width ω of cross-immunity 1 here. The mutation variance-covariance matrix for the change in antigenicity is isotropic in the two directions of the 2-dimensional antigenic space with the half of mutation variance (mutation rate times the squared width of mutation distance) $D = \mu m^2/2 = 0.01$. The half of mutation variance for the change in virulence is $D_\alpha = \mu_\alpha m_\alpha^2/2 = 0.04$.

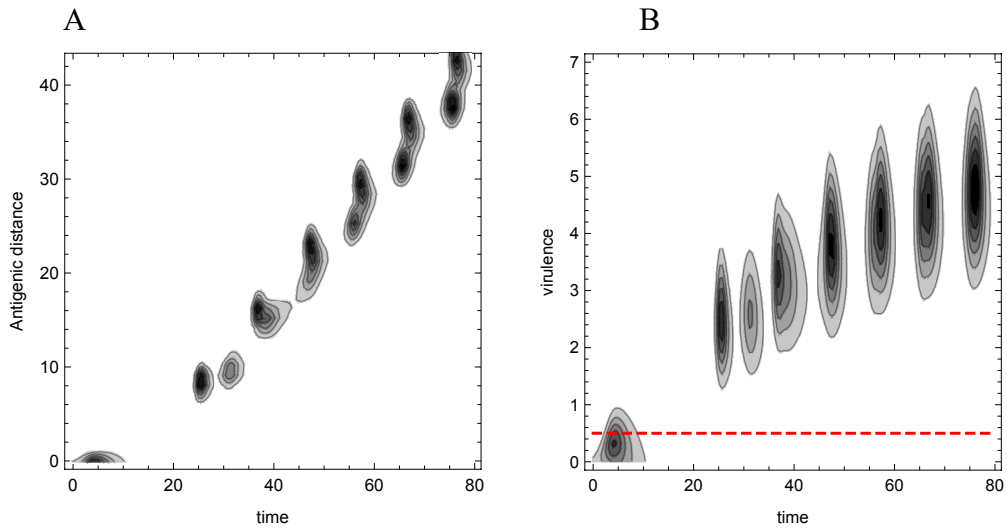

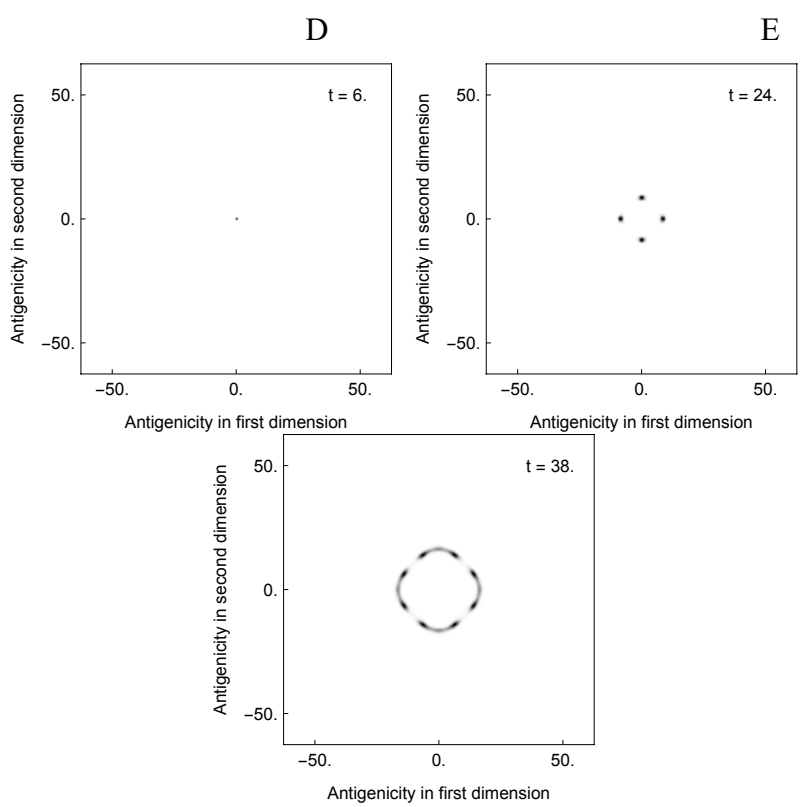

Supplementary Figure 2 The same as in Supplementary Figure 1 but with a wider width of cross-immunity, $\omega = 3$ (where $\omega = 1$). The snapshots are taken at time $t = 6$, 24, and 38 in C, D, and E.